MASARYKOVA UNIVERZITA
Přírodovědecká fakulta
Ústav teoretické fyziky a astrofyziky

Bakalářská práce

Brno 2025 Alona Lazarieva

MASARYKOVA
UNIVERZITA
PŘÍRODOVĚDECKÁ FAKULTA
ÚSTAV TEORETICKÉ FYZIKY A ASTROFYZIKY

Absolutní fotometrie otevřené hvězdokupy NGC 2099

Bakalářská práce

Alona Lazarieva

Vedoucí práce: RNDr. Jan Janík, Ph.D. Brno 2025

Bibliografický záznam

Autor:	Alona Lazarieva Přírodovědecká fakulta, Masarykova univerzita Ústav teoretické fyziky a astrofyziky
Název práce:	Absolutní fotometrie otevřené hvězdokupy NGC 2099
Studijní program:	Fyzika
Studijní obor:	Astrofyzika
Vedoucí práce:	RNDr. Jan Janík, Ph.D.
Akademický rok:	2024/2025
Počet stran:	VII + 57
Klíčová slova:	otevřená hvězdokupa NGC 2099; absolutní fotometrie; barevné diagramy; extinkce

Bibliographic Entry

Author:	Alona Lazarieva Faculty of Science, Masaryk University Department of Theoretical Physics and Astrophysics
Title of Thesis:	Absolute photometry of open cluster NGC 2099
Degree Programme:	Physics
Field of Study:	Astrophysics
Supervisor:	RNDr. Jan Janík, Ph.D.
Academic Year:	2024/2025
Number of Pages:	VII + 57
Keywords:	open cluster NGC 2099; absolute photometry; color diagrams; extinction

Abstrakt

Cílem této práce je provést CCD fotometrii otevřené hvězdokupy NGC 2099 a na základě získaných pozorovacích dat určit její základní parametry. Teoretická část zahrnuje přehled hvězdokup, popis Hertzsprungova-Russellova diagramu, základy fotometrie a principy CCD kamer, jakož i obecné informace o hvězdokupě NGC 2099. Praktická část je věnována pozorování, zpracování získaných dat a analýze výsledků.

Na základě sestavených diagramů barva-magnituda bylo možné určit vzdálenost k hvězdokupě, její věk a chemické složení. Na závěr byly získané údaje porovnány s výsledky prezentovanými v odborné literatuře.

Abstract

The purpose of this work is to perform CCD photometry of the open cluster NGC 2099 and determine its fundamental parameters based on the obtained observational data.

The theoretical part includes an overview of star clusters, a description of the Hertzsprung–Russell diagram, the basics of photometry and the principles of CCD cameras, as well as general information about the cluster NGC 2099. The practical part is devoted to the observations, processing of the obtained data, and analysis of the results.

Based on the constructed color-magnitude diagrams, it was possible to determine the distance to the cluster, its age, and chemical composition. In conclusion, the obtained data were compared with the results presented in the scientific literature.

MUNI
SCI

MASARYKOVA UNIVERZITA
FACULTY OF SCIENCE
KOTLÁŘSKÁ 2, 611 37 BRNO
IČ: 00216224
DIČ: CZ00216224

BACHELOR'S THESIS DESCRIPTION

Academic year: 2024/2025

Department:	Department of Theoretical Physics and Astrophysics
Student:	Alona Lazarieva
Programme:	Physics
Specialization:	Astrophysics

In compliance with the Study and Examination Regulations of Masaryk University, the Department Head of *ústavu* at the Faculty of Science, MU is assigning you a Bachelor's thesis with the title:

Title of the thesis/dissertation:	Absolutní fotometrie otevřené hvězdokupy NGC 2099
Title of the thesis in English:	Absolut photometrz of open cluster NGC 2099
Language used:	English

Final Description:
Na základě vlastních měření ve fotometrických filtrech UBVRI otevřené hvězdokupy NGC 2099 student získá standardizované jasnosti hvězd v hvězdokupě, zkonstruuje její barevný diagram, určí parametry hvězdokupy a mezihvězdnou extinkci ve směru k hvězdokupě. Porovná zjištěné parametry s daty z astrometrické družice GAIA a dalších zdrojů.

On the basis of their own measurements in the UBVRI photometric filters of the open cluster NGC 2099, the student will obtain standardized magnitudes of the stars in the cluster, construct a color diagram of the cluster, determine the cluster parameters and the interstellar extinction in the direction of the cluster. Compare the determined parameters with data from the GAIA astrometric satellite and other sources.

Thesis supervisor:	RNDr. Jan Janík, Ph.D.
Thesis assignment date:	2025/02/19
In Brno, date:	2025/05/12

The description was approved through IS MU.

Alona Lazarieva, 2025/02/19
RNDr. Jan Janík, Ph.D., 2025/03/20
RNDr. Luboš Poláček, 2025/03/20

Poděkování

Ráda bych vyjádřila upřímnou vděčnost svému vedoucímu RNDr. Janu Janíkovi, Ph.D., za jeho neocenitelnou pomoc a podporu ve všech fázích psaní mé bakalářské práce a za trpělivost.

Prohlášení

Prohlašuji, že jsem svoji bakalářskou práci vypracovala samostatně pod vedením vedoucího práce s využitím informačních zdrojů, které jsou v práci citovány.

Brno 13. května 2025 .....

Alona Lazarieva

Contents

Introduction

If you look up at the night sky, you will probably recognize the characteristic figure of the Big Dipper or other most recognizable constellations. And while some stars in constellations may appear to be very close to each other, they may actually be separated by huge distances. Which is one of the main differences between constellations and star clusters. In clusters, stars are formed from one giant molecular cloud, so they are relatively close to each other and gravitationally bound, they have similar chemical composition, similar ages, and other identical properties. These characteristics of star clusters help us to learn when and where the processes of star formation took place and in what quantities, what was the content of heavy elements at that time and much more. In other words, we can reconstruct not only the history of our galaxy, but also better understand the universal and more general processes that occur in other galaxies and in the Universe as a whole. We can say that star clusters in a sense play the role of chroniclers of the history of galaxies and therefore they are an important tool in understanding and studying our universe.

Chapter 1

Star clusters

1.1 Formation of open star clusters

The formation of open star clusters begins with a giant molecular cloud. It consists mainly of hydrogen and helium, but may also contain some heavier elements or compounds. These gas and dust structures are truly unimaginable in size, with diameters ranging from a few tens to hundreds of light-years (Freedman et al., 2019).

The cloud itself is normally in hydrostatic equilibrium and is stable and homogeneous because the pressure of the gas balances the force of gravitational attraction. But some external events such as supernova explosion, collision of galaxies or clouds can lead to a shift in this balance and to the effect of gravitational instability, in consequence of which the density of the cloud becomes uneven and in places with higher density it begins to collapse, disintegrating into fragments.

During the compression process, these fragments still radiate energy and cool, but this happens until the density of the gas increases enough to make it nontransparent to radiation. After that, further fragmentation stops, and the already formed clots of gas begin to attract the remaining interstellar material to form accretion disks. Absorption of matter leads to an increase in temperature and subsequently to the beginning of thermonuclear reactions and complete evolution into a star.

Usually from one cloud can be formed from tens to several thousand stars that are gravitationally bound to each other, have a similar chemical composition and physical properties and are located at approximately the same distance from us, creating an open star cluster. However, in addition to open clusters, there are also globular clusters, whose formation and evolution process, as well as physical parameters are significantly different.

1.2 Globular clusters

Globular clusters usually contain a huge number of low-mass stars, sometimes reaching millions. These stars form a spherical structure about 60–150 light-years in diameter and their concentration increases toward the center of the cluster (Bennett et al., 2019).

Most globular clusters are located in the galaxy's halo, a spherical structure that surrounds the main visible part of the galaxy. This region has a lower density than the

galaxy disk, which makes it more stable and globular clusters can exist here for a very long time without collapsing or disintegrating.

Globular clusters typically consist of very old population II stars, which can be more than 10 billion years old, because they are thought to have probably formed soon after the Big Bang. This follows from the fact that the stars in these clusters are characterized by low metallicity, that is, they have a low content of heavy elements. Elements heavier than helium were synthesized in the cores of early stars and were ejected into space as a result of supernovae, after which they became the material for the formation of the next generation of new stars, which contain more heavy elements. From this we can conclude the age of clusters by the metallicity of their stars.

Thus globular clusters can tell us about ancient stars and the early evolution of galaxies and the universe, but they do not give us a complete understanding of all the processes. What about younger stars and their evolution? For this, we can look at a second type of star clusters — open clusters.

Figure 1.1: Globular cluster M2 [e2]

1.3 Open clusters

The first thing that catches the eye when comparing globular and open clusters is the difference in their shape. Open clusters have an irregular and chaotic structure typically about 30 light-years across with no clear symmetry (Bennett et al., 2019). The number of stars in them also differs noticeably, they can contain from a few tens to hundreds of thousands of stars, unlike globular clusters that can contain up to millions of low-mass stars.

Figure 1.2: Open cluster M45 [e3]

But appearance is not the only difference between them. Because of the lower population density, open clusters are not so strongly bound gravitationally, and as a consequence are unstable and stars can easily leave the cluster when interacting with other stars or clouds of gas, or even from the action of tidal forces of the galaxy. Because of this, they can decay rather quickly, and their lifetime varies from millions to hundreds of millions of years, but there may be exceptions of a billion years.

Another difference is that open clusters are quite young. They are usually located in the arms of spiral galaxies, where the gas density is high and star formation processes are still active today. However, this dynamic environment is the cause of their fast destruction. Although the open clusters are mostly in the disks of spiral galaxies, we can also see them in irregular galaxies, where new stars are still forming. But in elliptical galaxies they are

not observed, because in them star formation is no longer occurring, and those clusters that were there have long since disintegrated.

It is also worth mentioning a little about the classification of open clusters. Many types of classifications have been invented by different scientists, but currently the most commonly used is the Trumpler classification system, in which clusters are divided based on three visual and easily measurable parameters:

- Degree of Concentration:

  I. Detached clusters with strong central concentration.

  II. Detached clusters with little central concentration.

  III. Detached cluster with no noticeable concentration.

  IV. Clusters not well detached, but has a strong field concentration

- Range of Brightness

  1. Most of the cluster stars are nearly the same apparent brightness.
  2. A medium range of brightness between the stars in the cluster.
  3. Cluster is composed of bright and faint stars.

- Number of Stars in Cluster

  p. Poor clusters with less than 50 stars.

  m. Medium rich cluster with 50-100 stars.

  r. Rich clusters with over 100 stars.

Figure 1.3: The Trumpler classification [e4]

In conclusion, the stars of the open cluster formed from one giant molecular cloud at the same time, so that their properties such as age, chemical composition, and distance to us do not differ significantly and can be said to be the same for all stars in the cluster. This similarity of properties makes it much easier for us to study and analyze stars and their evolution. But also these stars have one important property that differs significantly — it is their mass.

Low-mass stars live much longer than higher-mass stars, which quickly use up their fuel, and as a result we have stars in the same cluster at different stages of evolution, even though they are all the same age. And although this difference might seem problematic at first, it actually helps us a lot when studying stars and the Hertzsprung-Russell diagram has become an effective tool for this purpose.

Chapter 2

Hertzsprung–Russell diagram

Temperature and luminosity are ones of the most accessible and easily measured parameters of stars and therefore it is not very surprising that two scientists independently from each other at around the same time came up with the idea to plot the dependence of these two quantities, which was later named in their honor the Hertzsprung-Russell diagram. To be a little more precise, Einar Hertzsprung made a diagram “color index - apparent magnitude”, and Henry Norris Russell — “spectral class - absolute magnitude”, and there may also be a diagram “temperature - luminosity”, but in general it is the same graph, because all these parameters are related to each other.

2.1 Structure and parameters of the H-R diagram

On the horizontal axis is usually plotted the effective surface temperature of the star, which is also closely related to the spectral class. As can be understood from the name, this classification is based on the spectra of stars with different absorption lines and their intensity, which in turn depend on temperature, as it affects the degree of excitation and the number of ionized atoms, which subsequently forms these characteristic absorption lines in the spectrum of the star.

Also, the temperature of the star determines its color index. Since the emission spectrum of a star is similar to the emission spectrum of an absolute black body, the Wien’s displacement law can be applied to it, according to which at high temperatures the maximum of the intensity of radiation shifts to shorter wavelengths. It turns out that in the blue filter B a hot star will look brighter than, for example, in the visible V and then its color index $(B-V)$ will have a small value. Conversely at low temperatures the color index will have a larger value.

Thus, temperature, spectral class and color index are related to each other, which are mainly used to represent the horizontal axis of the H-R diagram. It is also worth noting that historically, this axis has been in reverse order, i.e., hotter stars are on the left and cooler stars are on the right.

The vertical axis represents the luminosity of stars, i.e., the amount of energy emitted by a star per unit time. The luminosity can be determined by knowing the radiant flux of the star F and the distance to it r, using the formula:

$$L = 4\pi F r^2 \text{ [W]} \tag{2.1}$$

Also, knowing the effective temperature of the star, the Stefan-Boltzmann law can be used:

$$L = 4\pi R^2 \sigma T^4 \ [\mathrm{W}], \tag{2.2}$$

where $\sigma = 5.67 \cdot 10^{-8}$ $[\mathrm{Wm^{-2}K^{-4}}]$ is Stefan-Boltzmann constant, R is star's radius and T its temperature.

From this formula 2.2, we can also see that by knowing the temperature and luminosity of a star, we can calculate its radius. Thus, if stars have the same temperature, but different luminosity, they have different radii and the brighter star has a larger radius. Therefore, the H-R diagram also gives us information about the radii of the stars and it shows how the radii increase as we go from the lower left corner with high temperature and low luminosity to the upper right corner with low temperature and high luminosity.

But in addition to this, we can also see in the diagram that the stars are not uniformly distributed, but group several regions. This distribution shows us very well the evolution of the star.

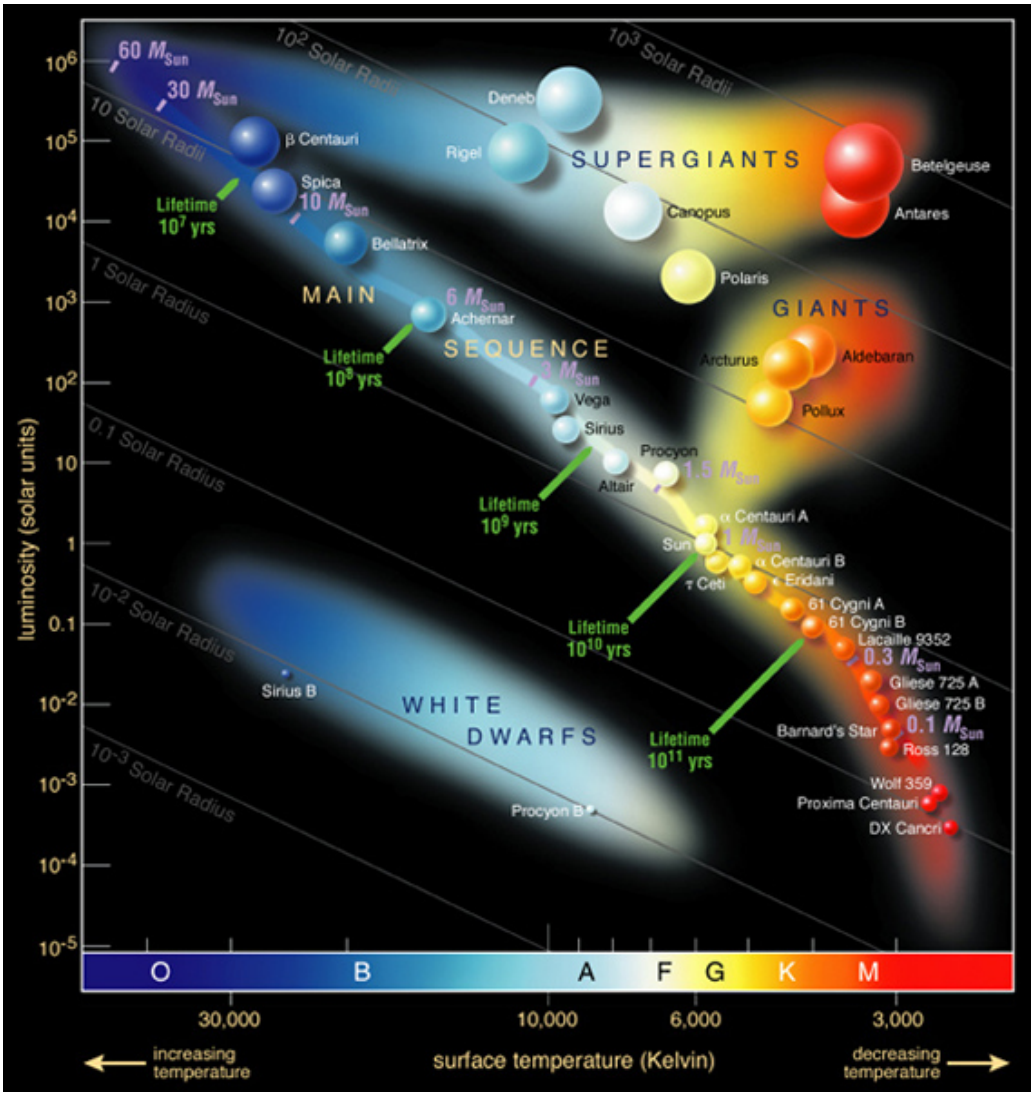

Figure 2.1: Hertzsprung–Russell diagram [e5]

2.2 Position of stars on the H-R diagram and their evolution

The most noticeable and populated group is the main sequence, which runs diagonally from the upper left corner with bright hot stars to the lower right corner with faint and cool stars. Here stars spend most of their lives burning hydrogen in their cores, which explains why this group is so numerous (90% of the universe's stellar population, including the Sun). The position of a star on this sequence depends mainly on its mass — the more massive the star, the hotter and brighter it is, and the higher it is on the main sequence. But such stars burn their hydrogen and evolve faster, so the upper part of the sequence is less populated than the lower part.

Once a star has run out of hydrogen, it begins more complex thermonuclear reactions, causing its brightness to increase and its outer shell to expand and its surface to cool. In the diagram, we see the star moving rightward and upward into the region of giants or supergiants — depending on its mass.

Solar-mass stars after the giant stage throw off the outer shell, forming a planetary nebula in the center of which remains a hot and compact core of this star — a white dwarf. Accordingly, in the diagram such a star moves to the lower left corner, where the region of white dwarfs is located.

The life cycle of massive stars ends differently. At the end of the supergiant stage occurs the supernova explosion and collapse of the core into a neutron star or black hole, which are not shown on the H-R diagram.

Thus the H-R diagram not only classifies stars, but can also quite clearly visualize the physical properties and evolution of stars, and is therefore very useful for studying open clusters.

2.3 H-R diagram of open clusters

Since the stars in the cluster were formed at about the same time from the same cloud and at the same distance from us, all the differences in brightness and evolution are due to differences in mass. The curve that connects in a diagram such stars of the same age but different masses, which are at different stages of evolution, is called the isochrone.

At first the isochrone follows the main sequence, but then, as massive stars evolve faster and move into the region of giants, the isochrone begins to bend strongly toward this region of low temperature and high luminosity. The place where this bending occurs is called the turnoff point. Over time, less massive stars begin to evolve into giants and the turnoff point falls lower and lower.

From this we can tell the age of the cluster by the position of the turnoff point. The younger the cluster, the fewer stars have had time to evolve to the giant stage and the higher the turnoff point. Conversely, the older the cluster is, the more giants there are in it and the turnoff point is lower.

Thus, the analysis of the observed diagram of a star cluster and its comparison with theoretically calculated isochrones allows us to know its main parameters, including its age, metallicity, distance to it and the stages of evolution of stars in it. But for this purpose,

it is necessary to first obtain photometric data, which will be the basis for further analysis.

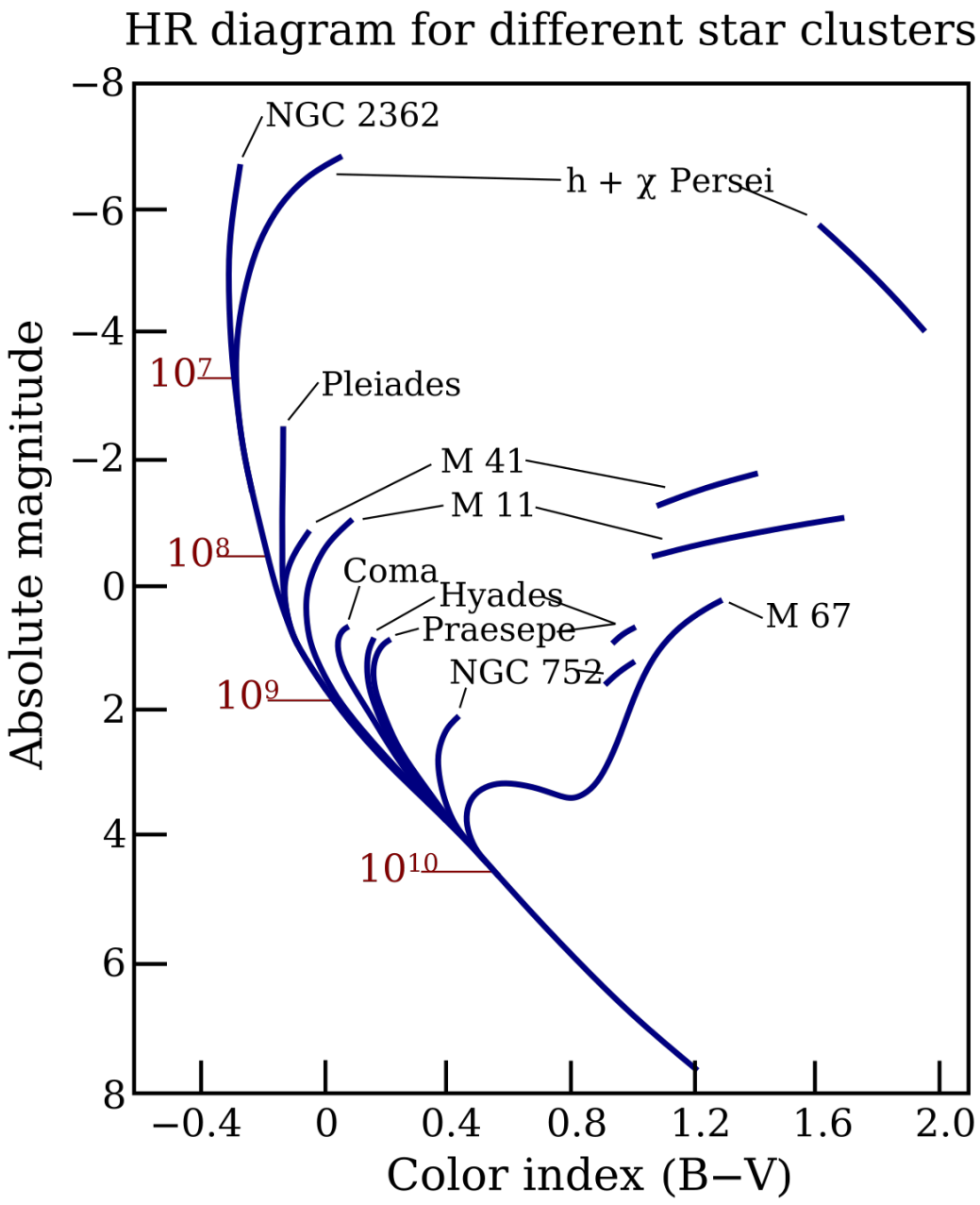

Figure 2.2: H-R Diagrams for different clusters [e6]

Chapter 3

Photometry

Most of the information about stars comes to us in the form of electromagnetic radiation. Because this radiation can travel freely in a vacuum, it is the main source of data on the physical parameters of stars. The field of astronomy that studies and measures these fluxes of radiation from cosmic objects is called photometry. It is one of the main methods of observational astronomy and allows us to calculate many physical characteristics of stars, including luminosity, temperature, chemical composition, distance to the objects, the influence of the interstellar environment, and more. But to do that, we must first understand basic photometric quantities such as stellar magnitudes and color indices.

3.1 Stellar magnitudes and color indices

To evaluate the brightness of astronomical objects, several interrelated stellar magnitudes are used in photometry. The main measured quantity is the apparent magnitude, which shows the brightness of an object in a specific filter as seen from Earth. It can be determined using the Pogson's equation:

$$m = -2{,}5 \log \left(\frac{F}{F_0} \right) \text{ mag}, \tag{3.1}$$

where F is the radiant flux from the star in a specific filter, F_0 is the radiant flux from a standard source in that filter, which sets the zero point of the scale.

However, this value depends not only on the radiant flux, but also on the distance to the object, and even a very bright star will appear faint if it is very far away from us. Therefore, to remove this dependence on distance and more accurately compare the brightness of stars, absolute magnitude is used. It is defined as the apparent magnitude that an object would have at a distance of 10 parsecs from the observer. Absolute magnitude is related to the apparent magnitude through the distance modulus:

$$m - M = 5 \log (r) - 5 \text{ mag}, \tag{3.2}$$

where r is the distance to the object in parsecs.

Thus, absolute magnitude characterizes the true brightness of objects and makes it possible to compare them more accurately.

In addition to magnitudes measured in a specific range of the spectrum, there is also bolometric magnitude, which covers the entire range of electromagnetic radiation. However, since it is very difficult to measure the flux in the entire electromagnetic spectrum in practice, a bolometric correction *BC* is used, which depends on the spectrum of the star's radiation and links the bolometric and apparent or absolute magnitudes:

$$BC = m_{bol} - V = M_{bol} - M_V \text{ mag} \tag{3.3}$$

It can be used to correct apparent or absolute magnitudes for analyzing the total luminosity of a star.

Another important characteristic is the color index. It represents the difference between two magnitudes measured in two different filters. As a rule, to calculate it, the value in the C_2 filter with a longer wavelength is subtracted from the value in the C_1 filter with a shorter wavelength:

$$CI = m(C_1) - m(C_2) \text{ mag} \tag{3.4}$$

As already mentioned in the chapter about the H-R diagram, the color index reflects the temperature of a star — for hot stars, it takes on lower or even negative values, while for cold stars, it is positive. In addition, color indices can be measured without knowing the distance to the star, which makes them especially useful for analyzing the physical parameters of stars based on photometric observations. But since color indices depend on observations in different spectral ranges, the photometric system used to set the filter parameters plays an important role.

3.2 Photometric systems

As mentioned earlier, it is very difficult in practice to measure the bolometric magnitude across the entire electromagnetic spectrum, so we determine the brightness of an object in specific wavelength ranges. For this purpose, photometric systems are used, which are based on sets of filters, each of which transmits radiation in a specific wavelength range.

The main purpose of photometric systems is to make brightness measurements of stars from different observations comparable. This allows for more accurate and reliable comparisons of data obtained by different instruments and under different conditions. For this purpose, each system uses specific filters, processing and calibration methods, and standard stars with precisely known magnitudes in each filter, with which the measured values are compared. In addition, an important characteristic of each filter is its bandwidth — the range of wavelengths to which the filter is sensitive. They are mainly divided into three types:

- Broadband ($>$ 30 nm) — pass a wide range of wavelengths and allow more light to be collected, which in turn increases sensitivity and speeds up the shooting process. However, this also means that different emission lines or different elements can enter the filter, making them less suitable for accurate spectral analysis.
- Medium band (10 - 30 nm) — intermediate between the broadband and narrowband. They are used when more accurate spectral data is required, as they are narrow

enough to isolate only the desired parts of the spectrum, but wide enough to maintain sensitivity.

- Narrowband (several nm) — conversely, they transmit radiation in a very narrow range and are almost monochromatic. They allow the spectral lines of radiation from specific chemical elements to be recorded.

There are many different photometric systems, but the most common and widely used is the Johnson's system, which consists of three basic filters:

- *U* (ultraviolet) — transmits in the range from 300 nm to 420 nm with a maximum at 360 nm.
- *B* (blue) — transmits in the range from 360 nm to 560 nm with a maximum at 420 nm.
- *V* (visible) — transmits in the range from 460 nm to 740 nm with a maximum at 535 nm.

Over time, this system was expanded to include the red and infrared regions of the spectrum by adding the *R* (700 nm) and *I* (900 nm) filters, respectively. The addition of these ranges expanded the capabilities of photometric observations and made it possible to study areas of dust and gas that had previously hidden the objects behind them, since longer wavelengths pass much better through interstellar dust, which absorbs short-wave radiation more strongly. Therefore, when analyzing data, it is also very important to take into account interstellar extinction, which can significantly distort the observed brightness of stars.

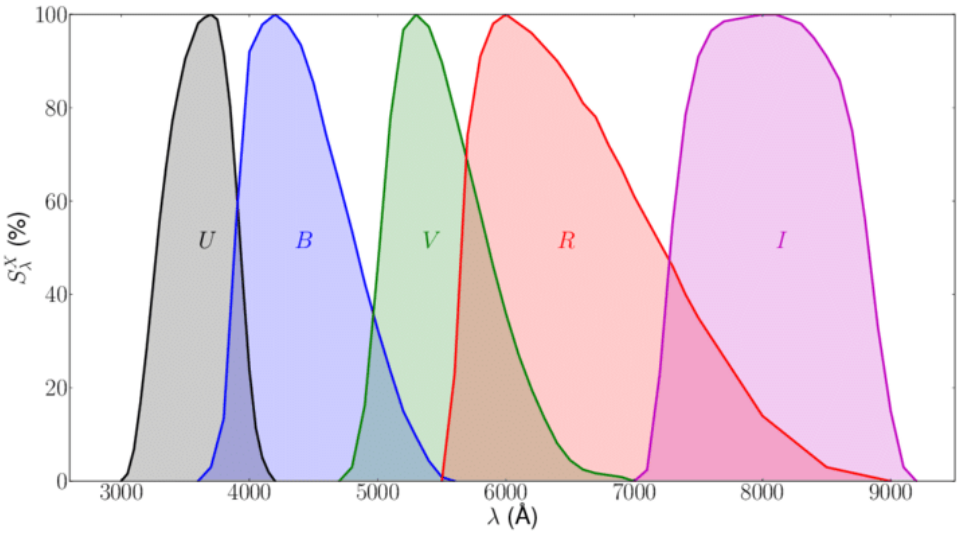

Figure 3.1: Sensitivity curves for the *UBVRI* filters [e7]

3.3 Interstellar extinction

When radiation from an object travels through space toward us, it encounters interstellar dust and gas particles that fill the space. These particles significantly affect the observed brightness and color of the star, as they selectively absorb and scatter its light. Selective absorption means that interstellar dust absorbs radiation differently at different wavelengths. Short-wavelength light, such as blue and ultraviolet, is absorbed more strongly than longer-wavelength light, such as red and infrared. As a result, the star appears "redder" than it actually is and, accordingly, colder, which can lead to errors in data analysis if this effect is not taken into account. This color change is called interstellar reddening, and color excess is used to quantify it. It is calculated as the difference between the observed color index and the true value, i.e., what it would be without the influence of interstellar extinction:

$$E(B-V) = (B-V)_{\text{observed}} - (B-V)_{\text{real}} \text{ mag} \tag{3.5}$$

In addition, there are numerical ratios that allow us to find the color excess or the amount of absorption in specific filters based on measured data in several filters. For example, for *UBVRI* filters, the ratios $E(\lambda - V)/E(B-V)$ or $A_\lambda/E(B-V)$ can be used. For example $A_V = R_V \cdot E(B-V)$, where R_V is the empirical mean coefficient in the visible range, which is approximately 3.1 for our galaxy.

The influence of interstellar absorption is also very clearly visible in color diagrams. In these diagrams, the observed values are shifted horizontally relative to the theoretical isochrones, which correspond to the values without absorption. The color excess can be determined from the distance between the observed values and the theoretical curve. Thus, by knowing the absorption values in different filters and the color excesses, it is possible to correct the observed data and obtain more accurate and correct information about the objects. However, even then, some inaccuracies may still remain, which are related to the operation of the measuring device — the CCD camera.

3.4 CCD and image calibration

In astronomical observations, the main instrument that records incoming radiation from space objects is a CCD matrix. Its principle of operation is based on the photoelectric effect in a semiconductor material. When light from a star hits the sensor, photons free electrons, which then collect in the sensor's pixels. This collected electric charge, which is proportional to the amount of light hitting a pixel, is then converted into a digital value representing its brightness.

However, various types of noise and interference can occur during recording, which affect the signal and distort it. This noise can come from the camera itself or from external sources.

One of the main types of noise is dark current. It occurs because the device heats up during operation and, as the temperature rises, electrons can gain enough energy to be freed, which results in a noise signal. The higher the temperature of the semiconductor, the greater the dark current, so the devices are cooled during observations to reduce the influence of dark current.

Another option for reducing dark current is to use dark frames. These are taken with the same exposure as the light frames, but with the aperture closed, so that only dark current signals and readout noise, which occurs during the process of reading charges and converting them into numerical values, are displayed in these frames. These frames are then subtracted from the images of the target object to remove the contribution of this extra noise.

Another cause of interference is that the sensitivity of different pixels in the matrix may vary slightly from one another, or vignetting may occur, resulting in unevenness and gradients in the images. To eliminate these defects, flat field correction is performed. For this purpose, flat frames of a uniformly illuminated field of view are taken, which are then normalized and applied to the main image, correcting and aligning the background.

Therefore, it is very important to take these noises into account and minimize them using calibration methods to improve the quality and accuracy of photometric measurements, which are then used to study and analyze the observed object — in this work, the open cluster NGC 2099.

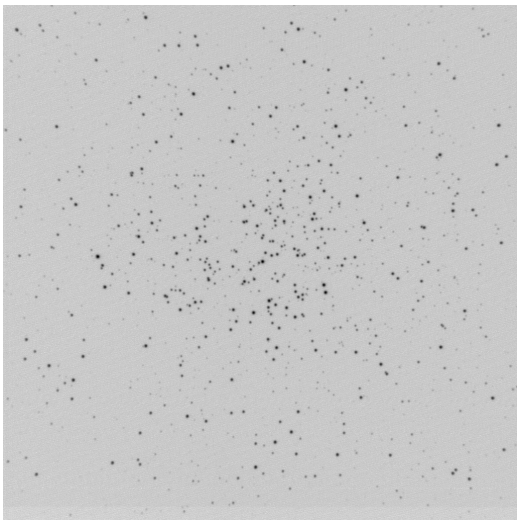

Figure 3.2: Raw image of NGC 2099 in the B filter

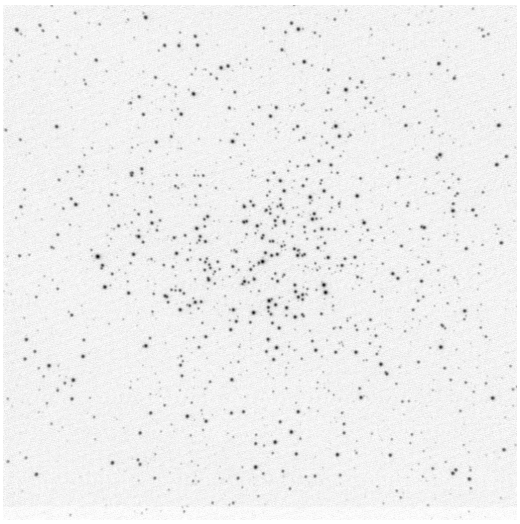

Figure 3.3: Processed image of NGC 2099 in the B filter

Chapter 4

Open cluster NGC 2099

4.1 Constellation Auriga and NGC 2099 observations

The object of this study is the open cluster NGC 2099, also known as M37. It is located in the constellation Auriga, which, according to ancient Greek mythology, was often associated with the hero Erichthonius, who first invented the two-wheeled chariot with four horses and used it in battle, as a result of which he became king of Athens. For his ingenuity and heroic deeds, Zeus placed him in the starry sky. The brightest star in the constellation Capella is associated with the goat Amalthea, that suckled Zeus.

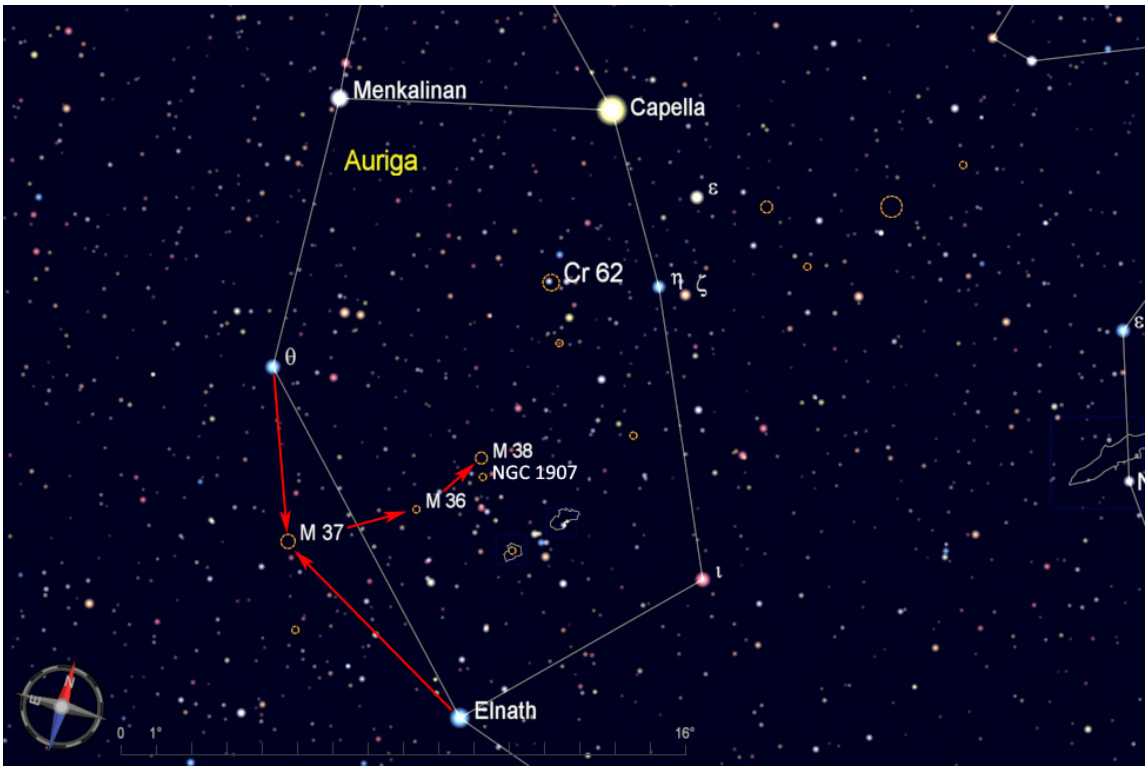

Figure 4.1: Constellation Auriga [e8]

Due to its high brightness, Capella is very visible in the northern hemisphere, especially in winter, making it a convenient starting point for searching for the M37 cluster. After finding Capella in the sky, move southeast toward the constellation Gemini. The cluster will be located slightly outside the characteristic pentagon of stars that form the asterism Auriga.

The cluster was first observed by Italian astronomer Giovanni Battista Hodierna before 1654. However, Guillaume Le Gentil did not notice it when he independently discovered the two neighboring clusters M36 and M38 in 1749, even though M37 is brighter than its neighbors. Therefore, it was independently "rediscovered" in September 1764 by Charles Messier, who added it to his famous catalog.

4.2 Characteristics and structure

Figure 4.2: Open cluster NGC 2099 [e9]

The NGC 2099 cluster is the largest and brightest of the three known open clusters in the constellation Auriga. Its equatorial coordinates are right ascension $5^{h}52^{m}18^{s}$ and declination $+32^{\circ}33'02''$ (J2000 epoch). Its apparent magnitude is about 6.2 mag.

It is also the most populated and is estimated to contain about 150 stars brighter than 12.5 mag, with a total of more than 500 stars. Its distance varies in different sources from approximately 1299 (Ferreira et al., 2025) to 2060 parsecs (Sarajedini et al., 2004).

Its angular size is about 24 arcminutes, which corresponds to a linear diameter of 20-25 light-years, depending on the distance assumed.

Estimates of the cluster's age also range from 300 million to 650 million years, making it quite old by astronomical standards. Its significant age is also indicated by the presence of a dozen red giants and the fact that the hottest main sequence star has a spectral class of B9V.

According to the Trumpler classification, the cluster is classified as I, 1, r or 1,2 r, which means that it is detached with a strong central concentration (I), with stars that have either almost the same apparent brightness (1) or a medium brightness range (2), and consisting of more than 100 stars (r).

4.3 Comparison with neighboring clusters

Near M37, also in the constellation Auriga, but inside the pentagonal asterism, there are two other open clusters — M36 and M38. Although all three clusters are located at approximately the same distance from Earth, they are at different stages of evolution.

The youngest cluster of the three is M36, estimated to be about 25 million years old and containing at least 60 stars, none of which are red giants.

M38 is older, about 220 million years old, and contains about 100 stars, including a yellow giant.

Figure 4.3: Open cluster M36 [e10]

Figure 4.4: Open cluster M38 [e11]

M37 is a quite old cluster containing a large number of stars, including red giants, which makes it especially interesting for research and analysis, which will be discussed in the practical part.

Chapter 5

Practical part

5.1 Observations and obtained images

Observations of the cluster NGC 2099 were made at the Suhora Observatory in Poland, which is located at latitude 49°34′09″ N, longitude 20°04′03″ E and altitude 1000 m, during four nights in January and one in March 2025. The detector was an Apogee Aspen-47 CCD camera. The data were taken in five *UBVRI* filters. The table 5.1 contains information about the number of images in each filter and their exposures.

Filter	Number of images	Exposure $[s]$
U	164	60
B	91 / 73	10 / 5
V	91/ 73	10 / 5
R	73 / 10 / 81	2 / 3 / 5
I	73 / 10 / 81	2 / 3 / 5

Table 5.1: Number of images for each filter with exposure times.

5.2 Data processing

The obtained images were processed in the SIPS (Scientific Image Processing System) program, where first calibration was made with dark frame and then with flat field. The proper measurement parameters had to be entered into the program, after what photometry and matching of stars with the UCAC4 catalog were performed. The result was a table containing all available information about the detected stars, including the equatorial coordinates, the name in this catalog, and the observed magnitudes in the corresponding filters. The resulting instrumental magnitudes were then compared with the standard stars from Landolt (2013) to correct and convert to the standard system, using the HEC22 program (Harmanec & Horn, 1998).

Since NGC 2099 is close to the plane of our galaxy, many stars from the galactic disk could also be in the frame, so it was necessary to determine which objects were most likely to belong to the observed cluster. At the first stage I removed stars for which there were

less than 10 measurements. Then I compared the remaining stars with data from the Gaia catalog and obtained values of their parallaxes and G magnitudes. Using this information, I left the stars whose parallaxes fell within a certain range corresponding to the belonging of NGC 2099. Then I plotted the dependence of the G magnitude on the color indices and additionally removed the stars that deviated significantly from the evolutionary path of the cluster.

The magnitudes obtained in different filters and color indices are presented in tables 5.4 and 5.5 in the appendix.

5.3 Color diagrams

After these calibration and correction steps, I have constructed color diagrams showing the dependence of magnitude V on the color indices $(B-V)$, $(U-B)$ $(V-R)$, $(V-I)$, and $(B-V)$ on $(U-B)$. These diagrams show very well the main sequence, the turnoff point, and the giants branch. In addition, diagrams with measurement errors of color indices and magnitude V are also presented.

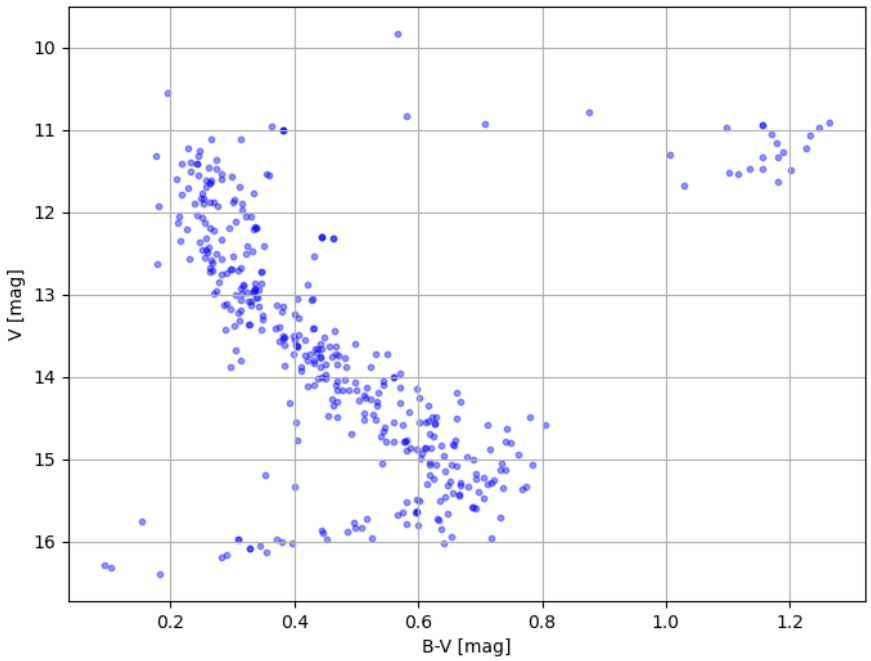

Figure 5.1: Color diagram of NGC 2099 for color index $(B-V)$

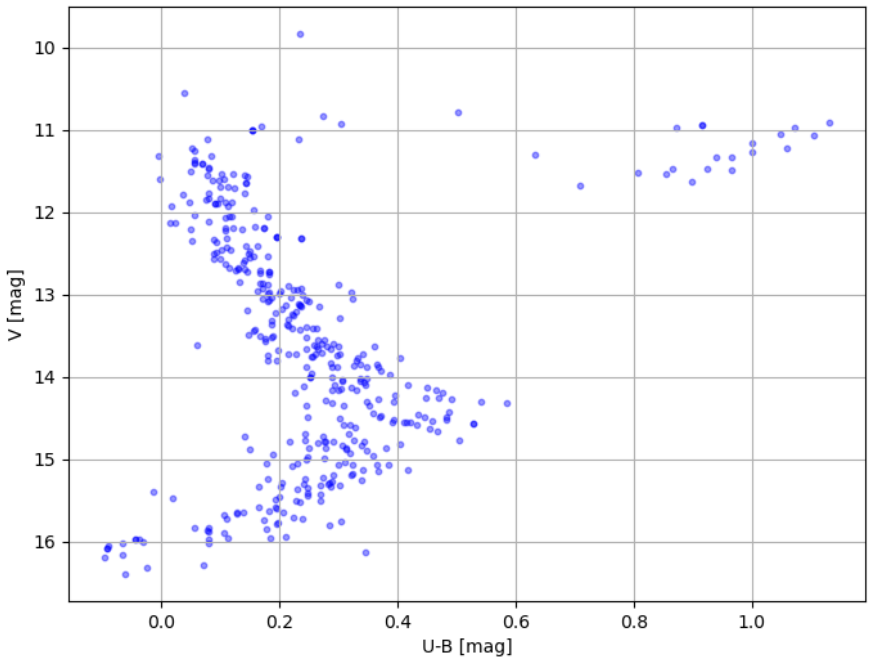

Figure 5.2: Color diagram of NGC 2099 for color index $(U-B)$

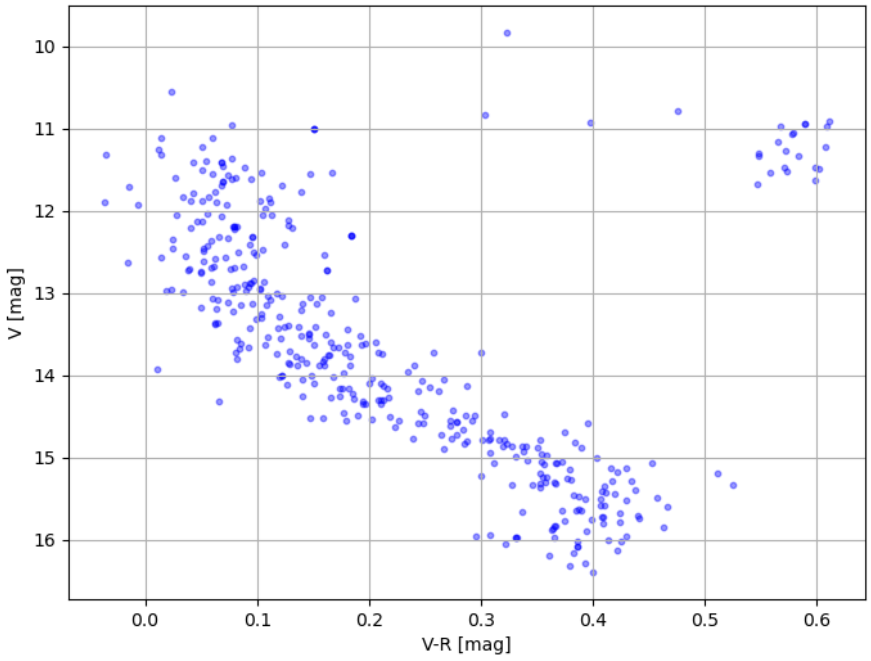

Figure 5.3: Color diagram of NGC 2099 for color index $(V-R)$

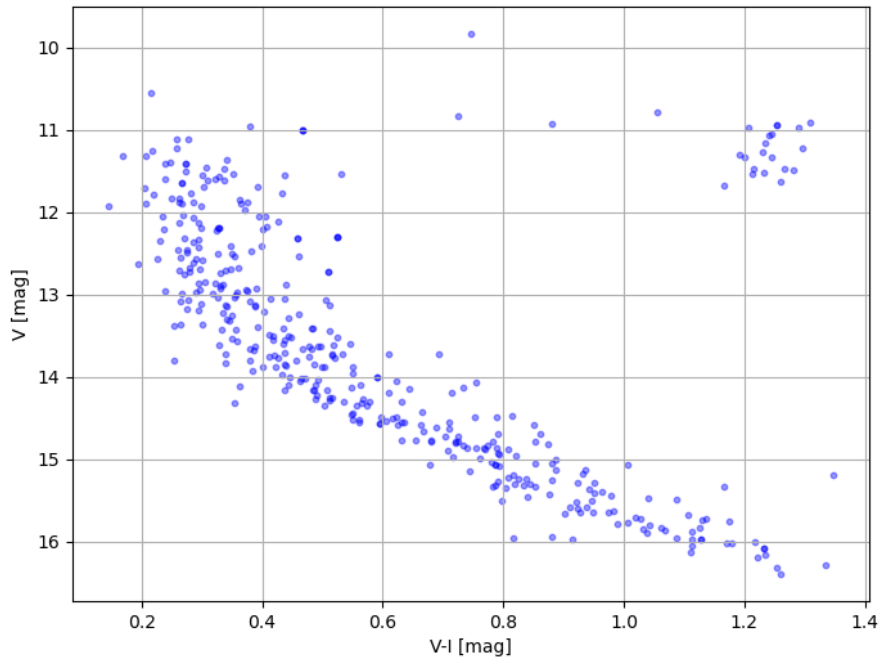

Figure 5.4: Color diagram of NGC 2099 for color index $(V-I)$

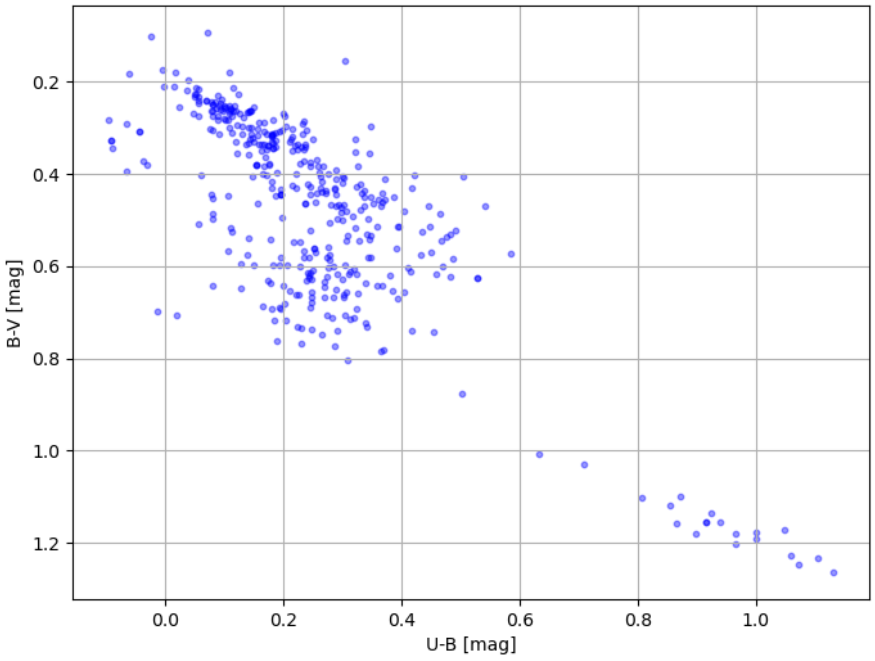

Figure 5.5: Color diagram of NGC 2099 for color indices $(B-V)$ and $(U-B)$

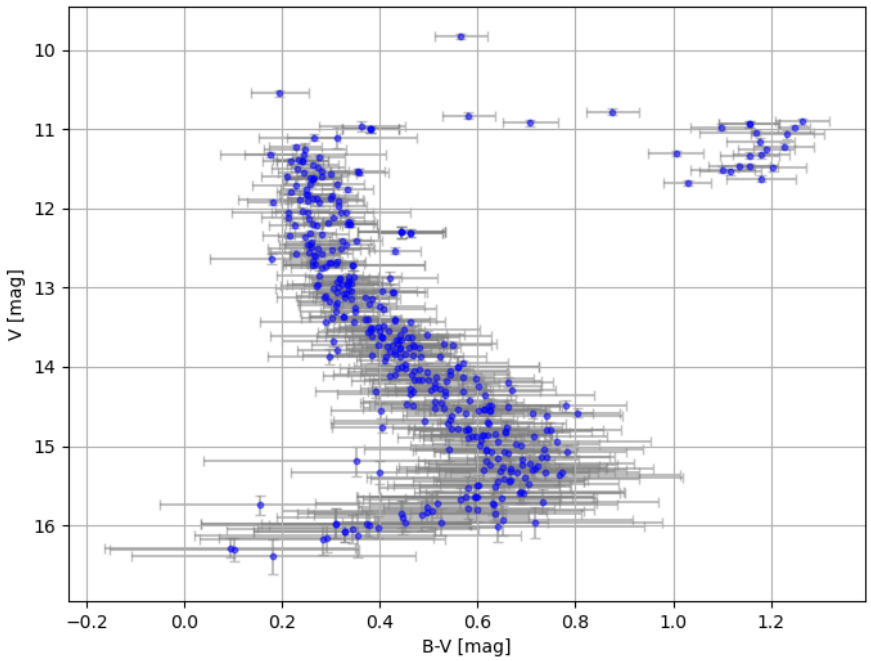

Figure 5.6: Color diagram of NGC 2099 with errors of color index $(B-V)$ and magnitude V

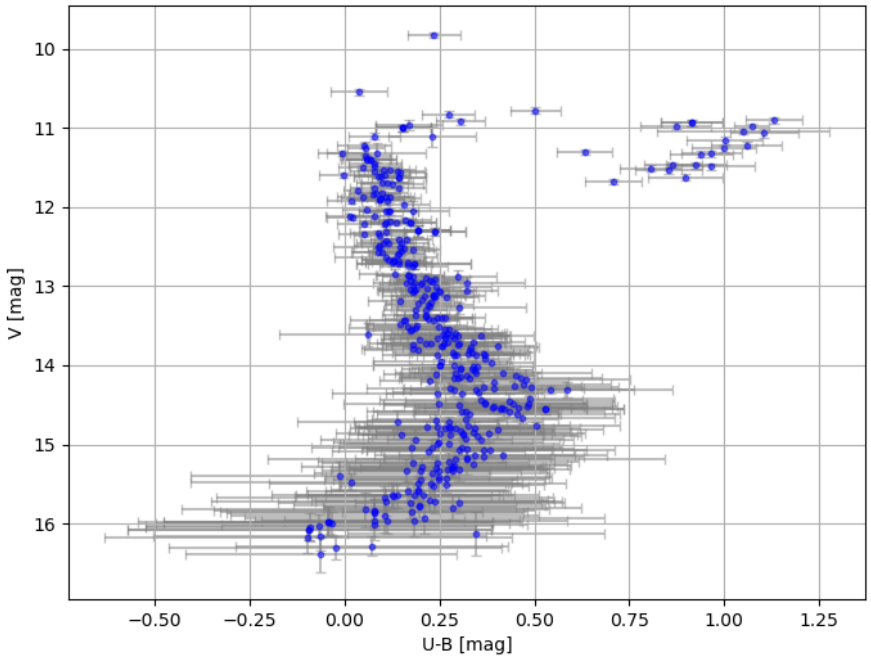

Figure 5.7: Color diagram of NGC 2099 with errors of color index $(U-B)$ and magnitude V

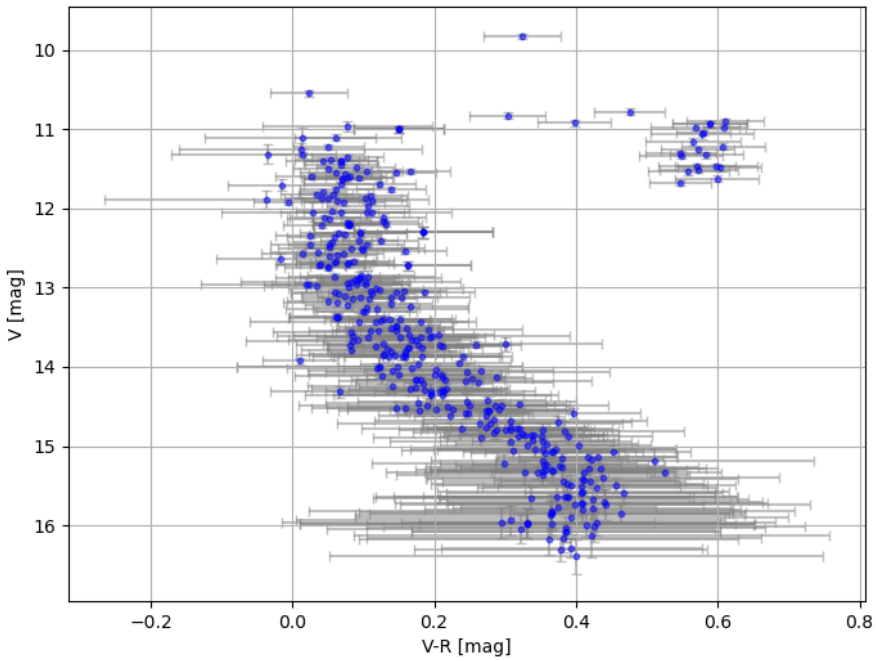

Figure 5.8: Color diagram of NGC 2099 with errors of color index $(V - R)$ and magnitude V

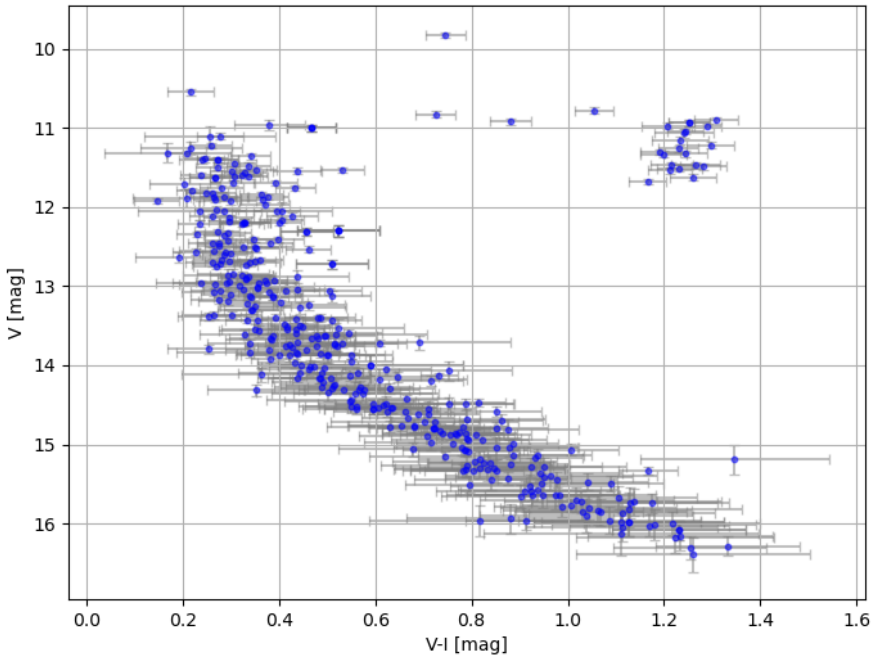

Figure 5.9: Color diagram of NGC 2099 with errors of color index $(V - I)$ and magnitude V

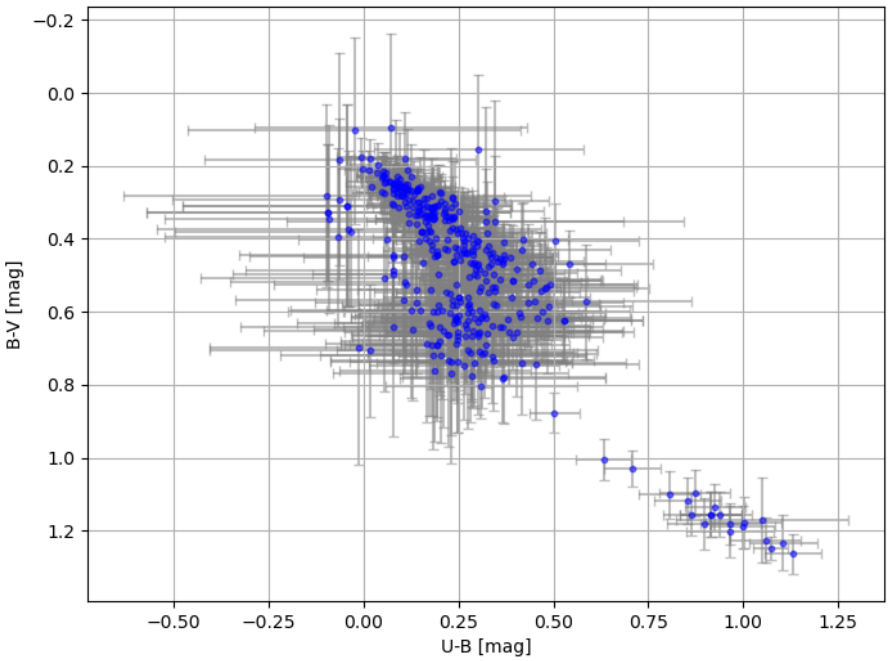

Figure 5.10: Color diagram of NGC 2099 with errors of color indices $(B-V)$ and $(U-B)$

5.4 Calculation of interstellar extinction

It was also important to calculate the values of interstellar extinction and color excesses. For this I used the method from the thesis Velčovský (2016), which is based on minimizing the differences between the measured color indices. The data from the table 5.2, presented in Savage et al. (1979), was used to determine the relationship between color excesses.

Filter	$\frac{E(\lambda-V)}{E(B-V)}$	$\frac{A_\lambda}{E(B-V)}$
U	1.73	4.75
B	1.00	4.10
V	0.00	3.10
R	-0.78	2.32
I	-1.60	1.50

Table 5.2: Interstellar extinction values for the Johnson-Cousin photometric system

From the table 5.2 we can obtain correlations between the interstellar absorption A_V in the V filter and the color excesses:

$$A_V = 1.79\,E(U-V) = 3.1\,E(B-V) = 2.42\,E(V-R) = 4.96\,E(V-I)\ \text{[mag/kp]} \quad (5.1)$$

Using the measured color indices and the equation 5.1, the least squares method was used to find such a value of A_V at which the differences between the color indices are

minimal. By this method, the value of the interstellar absorption in the V filter was found to be $A_V = 1.167 \pm 0.060$ mag/kpc. Then this value was used to find the color excesses:

$$E(B-V) = 0.377 \pm 0.019 \text{ mag}$$
$$E(V-R) = 0.294 \pm 0.015 \text{ mag}$$
$$E(V-I) = 0.603 \pm 0.031 \text{ mag}$$
$$E(U-B) = 0.271 \pm 0.014 \text{ mag}$$

The diagram 5.11 shows the differences between the color indices corrected for interstellar absorption. The values of $(V-R)$, $(V-I)$ and $(U-B)$ were converted to $(B-V)$ according to equation 5.1.

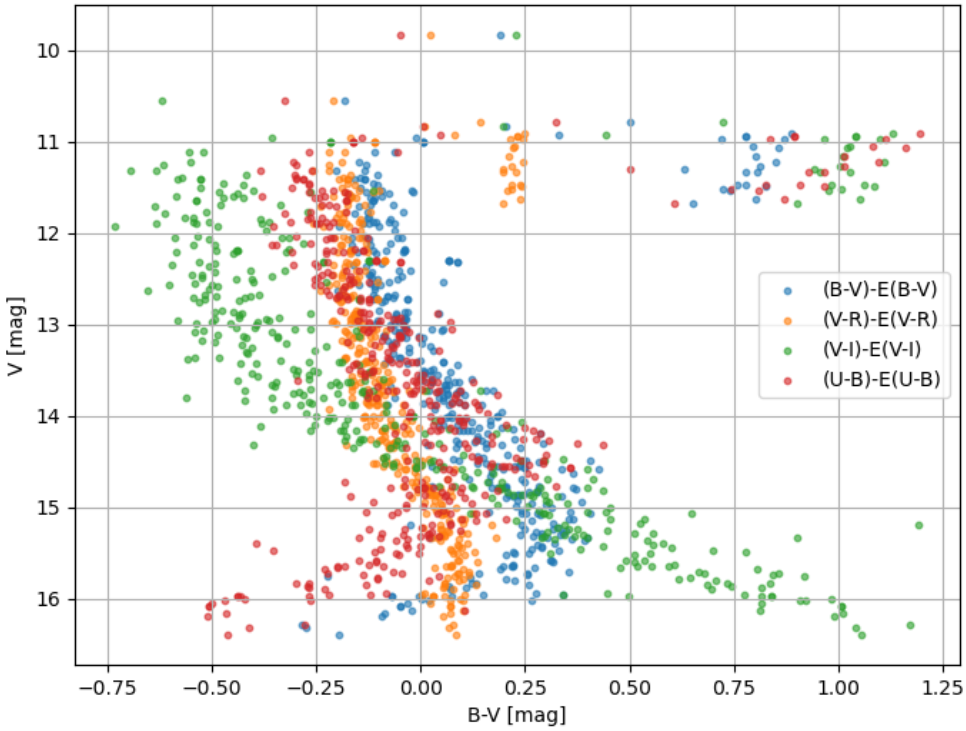

Figure 5.11: *UBVRI* color indices diagram corrected for interstellar extinction

5.5 Determination of age and metallicity

In order to determine the age of the cluster and its metallicity, it is necessary to compare the obtained color diagrams with theoretical isochrones. In this work I used theoretical isochrones from the database [e1], specifically from Bertelli et al. (1994).

Since the theoretical isochrones use absolute stellar magnitude and don't include the influence of interstellar absorption, I needed to transform my observed data correspondingly. For this purpose I used the formula 3.2, for which I calculated the distance equal

to $r = 1517 \pm 55$ pc from the parallax values, and also took into account the previously calculated color excesses and the value of the interstellar absorption A_V.

In the process of fitting, I determined that for my measurements the best fit for the model with age $10^{8.5}$ years, metallicity $Z = 0.008$ and $Y = 0.25$, which means that the age of the cluster is 316 million years and it contains 0.8% heavy elements, 25% helium and the remaining 74.2% are hydrogen.

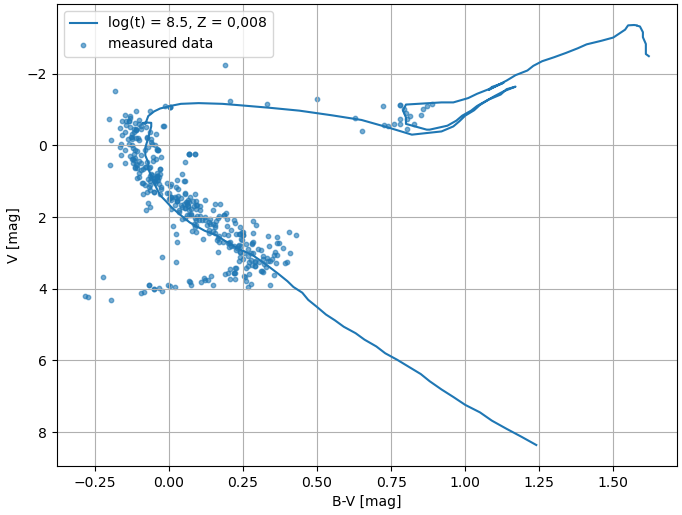

Figure 5.12: Color diagram of NGC 2099 and theoretical isochrone for the $(B-V)$ color index

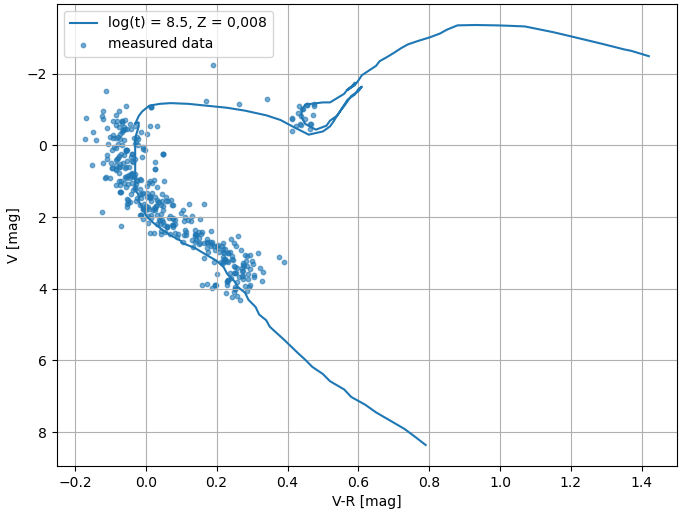

Figure 5.13: Color diagram of NGC 2099 and theoretical isochrone for the $(V-R)$ color index

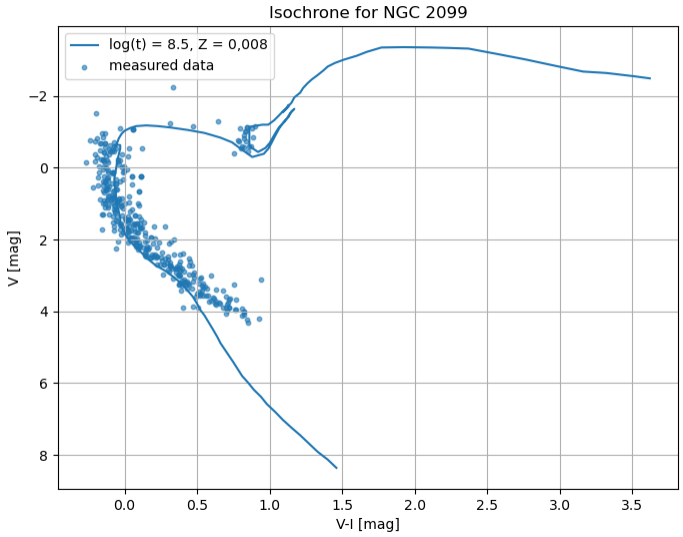

Figure 5.14: Color diagram of NGC 2099 and theoretical isochrone for the $(V-I)$ color index

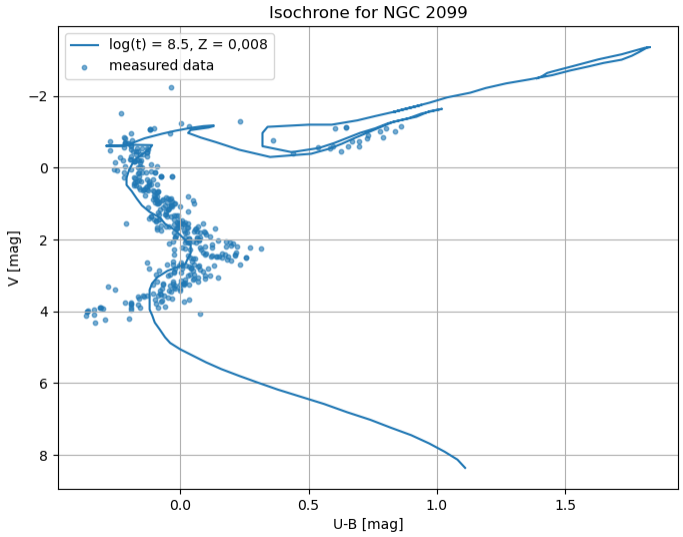

Figure 5.15: Color diagram of NGC 2099 and theoretical isochrone for the $(U-B)$ color index

The diagrams with color indices $(B-V)$ and $(U-B)$ initially matched the theoretical isochrones well, but the diagrams with color indices $(V-R)$ and $(V-I)$ were slightly shifted horizontally. This indicates that the color excesses for these indices were not calculated correctly. By selection of values and analysis of diagrams, I have determined that the best agreement of my data with theoretical data is at color excesses $E(V-R) = 0.135$ mag and $E(V-I) = 0.41$ mag. After that, using these obtained values, I have reconstructed the diagram of differences between color indices with correction for interstellar absorption and it began to look more unified.

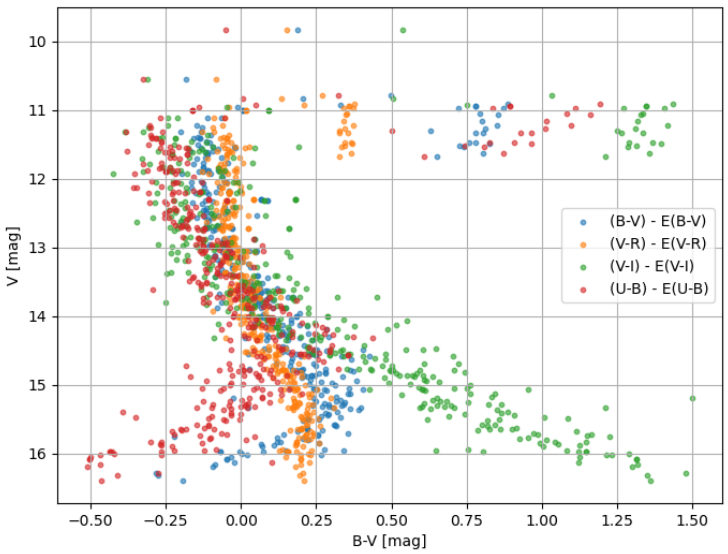

Figure 5.16: *UBVRI* color indices diagram corrected for interstellar extinction

5.6 Discussion of results

Based on the photometric data, I plotted the color diagrams, which show very well the main sequence, the turnoff point and the giants branch. Then comparing them with theoretical models I determined the age of the cluster to be 316 million years and the metallicity $Z = 0.008$. I also calculated the interstellar absorption in the V filter $A_V = 1.167 \pm 0.060$ mag/kpc, color excess $E(B-V) = 0.377 \pm 0.019$ mag, distance $r = 1517 \pm 55$ pc, and distance modulus $V - M_V = 10.90 \pm 0.08$ mag. To see how well the obtained data matches the literature, here is a table with the results of other papers.

Paper	Z	r [pc]	t [Myr]	$E(B-V)$ [mag]
Kalirai et al. (2004)	0.011	1995	650	0.23
Sarajedini et al. (2004)	0.02	2060	-	0.27
Kiss et al. (2001)	-	1300	450	0.29
Kang et al. (2007)	-	1905	-	0.21
Mermilliod et al. (1995)	0.02	1995	447	0.29
Nilakshi and R. Sagar (2002)	0.008	1360	400	0.30
West (1967)	0.02	1445	220	0.27
Ferreira et al. (2025)	0.02	1299	363	0.297
Casamiquela et al. (2019)	0.02	1440	400	-
this thesis	0.008	1517 ± 55	316	0.377 ± 0.019

Table 5.3: Comparison of parameters of open cluster NGC 2099

As can be seen from the table 5.3, my results generally fit well within the range obtained by other authors.

Summary

Over five nights, images of an open cluster NGC 2099 were obtained in five *UBVRI* filters. After image processing, color calibration, and calculation of interstellar absorption, I constructed color diagrams showing the dependence of magnitude V on the color indices $(B-V)$, $(U-B)$, $(V-R)$, $(V-I)$, and $(B-V)$ on $(U-B)$, which I used to determine the age and chemical composition of the cluster.

The age of the cluster NGC 2099 was determined to be 316 million years and the metallicity $Z = 0.008$, which is within the range reported in other studies. In addition, the distance to the cluster $r = 1517 \pm 55$ pc, the distance modulus $V - M_V = 10.90 \pm 0.08$ mag, the interstellar extinction in the V filter $A_V = 1.167 \pm 0.060$ mag/kpc and the color excess $E(B-V) = 0.377 \pm 0.019$ mag were calculated, which also correspond to the values reported in scientific papers.

In conclusion, the results of this study are consistent with existing theoretical data on the cluster NGC 2099, providing additional estimates of its age, distance, chemical composition, and interstellar extinction that can be used in further research.

Appendix

Table 5.4: Color indices with errors

star	$(B-V)$	$\sigma_{(B-V)}$	$(U-B)$	$\sigma_{(U-B)}$	$(V-R)$	$\sigma_{(V-R)}$	$(V-I)$	$\sigma_{(V-I)}$
900193	0.342	0.074	0.237	0.101	0.085	0.071	0.342	0.077
900195	1.030	0.049	0.708	0.074	0.547	0.043	1.166	0.038
900202	0.560	0.089	0.275	0.224	0.316	0.094	0.681	0.096
900212	0.226	0.054	0.050	0.070	0.041	0.053	0.236	0.048
900214	0.219	0.029	0.036	0.038	0.043	0.032	0.219	0.032
900220	0.436	0.093	0.272	0.147	0.128	0.085	0.437	0.065
900222	0.513	0.149	0.393	0.236	0.147	0.120	0.550	0.108
900230	0.580	0.143	0.348	0.276	0.267	0.153	0.708	0.141
900233	0.256	0.057	0.101	0.071	0.024	0.055	0.261	0.049
900234	0.264	0.053	0.120	0.063	0.041	0.052	0.263	0.045
900241	0.324	0.115	0.321	0.153	0.019	0.148	0.290	0.145
900242	0.270	0.074	0.200	0.084	0.034	0.075	0.267	0.074
900244	0.581	0.122	0.244	0.217	0.239	0.142	0.630	0.131
900247	0.561	0.165	0.252	0.175	0.122	0.201	0.591	0.193
900247	0.561	0.165	0.252	0.175	0.122	0.201	0.591	0.193
900251	0.383	0.094	0.258	0.155	0.086	0.108	0.328	0.094
900252	0.500	0.113	0.299	0.149	0.182	0.077	0.506	0.084
900253	0.635	0.156	0.269	0.256	0.407	0.139	0.797	0.134
900257	0.463	0.150	0.353	0.227	0.195	0.131	0.502	0.150
900258	0.463	0.066	0.237	0.082	0.095	0.065	0.458	0.055
900258	0.463	0.066	0.237	0.082	0.095	0.065	0.458	0.055
900259	0.180	0.052	0.016	0.065	-0.007	0.047	0.145	0.046
900263	0.246	0.084	0.056	0.049	0.012	0.171	0.217	0.106
900265	0.659	0.114	0.326	0.267	0.308	0.109	0.680	0.134
900269	0.344	0.257	-0.089	0.435	0.322	0.274	1.112	0.199
900270	0.524	0.095	0.244	0.146	0.240	0.070	0.550	0.085
900271	0.469	0.102	0.289	0.145	0.176	0.093	0.486	0.100
900274	0.182	0.291	-0.062	0.356	0.400	0.348	1.261	0.243
900275	0.715	0.150	0.312	0.302	0.389	0.117	0.770	0.155
900278	0.274	0.052	0.202	0.073	0.024	0.053	0.238	0.058
900281	0.446	0.258	0.105	0.405	0.394	0.305	1.038	0.222
900282	0.876	0.053	0.503	0.067	0.476	0.050	1.055	0.040

star	$(B-V)$	$\sigma_{(B-V)}$	$(U-B)$	$\sigma_{(U-B)}$	$(V-R)$	$\sigma_{(V-R)}$	$(V-I)$	$\sigma_{(V-I)}$
900285	0.270	0.054	0.107	0.065	0.080	0.051	0.323	0.046
900293	0.327	0.070	0.188	0.087	0.065	0.070	0.301	0.062
900301	0.574	0.196	0.139	0.269	0.385	0.242	0.949	0.160
900302	0.657	0.132	0.307	0.244	0.285	0.115	0.733	0.106
900304	0.406	0.077	0.147	0.089	0.146	0.062	0.412	0.065
900305	0.282	0.055	0.089	0.075	0.074	0.050	0.293	0.048
900307	0.391	0.124	0.289	0.135	0.066	0.097	0.353	0.101
900309	1.190	0.057	1.000	0.084	0.572	0.051	1.230	0.042
900310	0.212	0.054	0.014	0.063	0.046	0.050	0.262	0.047
900311	0.478	0.082	0.330	0.109	0.216	0.082	0.436	0.082
900314	0.249	0.056	0.080	0.067	0.034	0.050	0.262	0.048
900317	0.648	0.196	0.129	0.259	0.337	0.223	0.902	0.164
900319	0.667	0.158	0.270	0.270	0.411	0.127	0.876	0.130
900320	0.432	0.091	0.195	0.143	0.160	0.077	0.457	0.069
900321	0.598	0.195	0.182	0.233	0.387	0.178	0.982	0.154
900323	0.544	0.118	0.306	0.155	0.266	0.101	0.623	0.092
900324	0.597	0.117	0.304	0.155	0.254	0.084	0.645	0.088
900328	0.417	0.075	0.264	0.123	0.121	0.065	0.417	0.055
900329	0.330	0.061	0.179	0.082	0.111	0.060	0.380	0.064
900337	0.313	0.074	0.182	0.092	0.060	0.063	0.278	0.061
900338	0.546	0.100	0.327	0.241	0.273	0.101	0.688	0.100
900339	0.335	0.069	0.163	0.088	0.102	0.063	0.375	0.066
900340	0.624	0.105	0.273	0.248	0.278	0.095	0.724	0.092
900342	0.444	0.213	0.077	0.404	0.365	0.256	1.068	0.180
900349	0.297	0.067	0.205	0.083	0.050	0.057	0.276	0.059
900352	0.468	0.093	0.541	0.222	0.213	0.071	0.535	0.083
900353	0.580	0.122	0.343	0.276	0.301	0.119	0.725	0.122
900354	0.342	0.080	0.231	0.091	0.078	0.075	0.295	0.069
900355	0.566	0.202	0.106	0.445	0.424	0.218	1.106	0.161
900357	0.376	0.104	0.175	0.115	0.082	0.110	0.357	0.081
900359	0.331	0.057	0.120	0.072	0.113	0.052	0.395	0.048
900363	0.228	0.054	0.051	0.071	0.051	0.050	0.258	0.044
900365	0.420	0.096	0.300	0.099	0.093	0.117	0.439	0.106
900367	0.336	0.060	0.167	0.083	0.059	0.064	0.322	0.066
900368	0.601	0.131	0.470	0.232	0.141	0.119	0.516	0.112
900373	1.155	0.061	0.940	0.083	0.548	0.059	1.199	0.049
900374	0.735	0.204	0.231	0.317	0.372	0.167	0.879	0.144
900375	0.398	0.080	0.189	0.135	0.146	0.080	0.442	0.061
900376	0.443	0.083	0.245	0.144	0.173	0.078	0.481	0.067
900377	0.265	0.055	0.079	0.068	0.060	0.057	0.277	0.048
900378	0.404	0.076	0.299	0.137	0.107	0.073	0.387	0.060
900382	0.313	0.081	0.180	0.136	0.082	0.069	0.253	0.084
900383	0.431	0.053	0.181	0.069	0.160	0.057	0.461	0.047
900386	0.661	0.113	0.301	0.198	0.218	0.141	0.616	0.097

star	$(B-V)$	$\sigma_{(B-V)}$	$(U-B)$	$\sigma_{(U-B)}$	$(V-R)$	$\sigma_{(V-R)}$	$(V-I)$	$\sigma_{(V-I)}$
900387	0.400	0.182	0.165	0.141	0.328	0.196	0.853	0.152
900389	0.263	0.055	0.109	0.072	0.082	0.052	0.327	0.049
900390	0.441	0.096	0.271	0.149	0.165	0.089	0.435	0.098
900393	0.358	0.059	0.140	0.069	0.147	0.056	0.438	0.050
900394	0.513	0.147	0.359	0.268	0.246	0.154	0.551	0.177
900398	0.516	0.116	0.322	0.175	0.212	0.088	0.548	0.091
900400	0.497	0.076	0.291	0.136	0.206	0.078	0.546	0.069
900401	1.248	0.033	1.072	0.045	0.609	0.029	1.290	0.028
900403	0.334	0.063	0.182	0.085	0.089	0.065	0.358	0.058
900404	0.196	0.058	0.038	0.076	0.024	0.055	0.216	0.047
900406	0.452	0.128	0.079	0.238	0.332	0.179	0.913	0.126
900408	0.781	0.124	0.369	0.267	0.287	0.105	0.789	0.101
900410	0.324	0.057	0.143	0.075	0.094	0.054	0.348	0.054
900414	1.202	0.071	0.966	0.115	0.603	0.059	1.282	0.048
900416	0.570	0.092	0.254	0.180	0.235	0.073	0.550	0.085
900417	0.615	0.222	0.246	0.281	0.196	0.179	0.557	0.174
900418	0.441	0.094	0.257	0.148	0.163	0.077	0.412	0.083
900421	1.170	0.116	1.049	0.227	0.579	0.038	1.244	0.037
900422	0.313	0.162	0.232	0.115	0.014	0.139	0.257	0.136
900423	0.407	0.107	0.301	0.177	0.120	0.129	0.444	0.096
900425	0.309	0.058	0.166	0.067	0.077	0.067	0.339	0.063
900426	0.466	0.095	0.281	0.152	0.181	0.091	0.477	0.082
900430	0.536	0.195	0.476	0.277	0.243	0.178	0.609	0.182
900431	0.656	0.176	0.404	0.279	0.384	0.168	0.875	0.146
900432	0.451	0.134	0.348	0.145	0.120	0.128	0.472	0.092
900435	0.262	0.053	0.079	0.069	0.069	0.052	0.308	0.044
900436	0.690	0.208	0.194	0.232	0.410	0.206	0.937	0.165
900438	0.260	0.054	0.110	0.069	0.056	0.057	0.293	0.047
900440	0.331	0.054	0.149	0.072	0.105	0.051	0.381	0.048
900441	0.354	0.334	0.346	0.340	0.422	0.335	1.110	0.286
900446	0.179	0.126	0.108	0.136	-0.016	0.092	0.193	0.091
900447	0.338	0.056	0.172	0.069	0.079	0.051	0.328	0.052
900447	0.338	0.056	0.172	0.069	0.079	0.051	0.328	0.052
900451	0.246	0.055	0.093	0.068	0.058	0.066	0.285	0.043
900453	0.451	0.093	0.337	0.160	0.128	0.074	0.436	0.089
900454	0.668	0.194	0.284	0.244	0.435	0.148	0.923	0.146
900455	0.655	0.276	0.247	0.298	0.408	0.221	0.950	0.184
900457	0.213	0.116	0.115	0.078	0.104	0.120	0.406	0.104
900458	0.345	0.146	0.182	0.150	0.162	0.089	0.509	0.075
900458	0.345	0.146	0.182	0.150	0.162	0.089	0.509	0.075
900459	0.244	0.170	0.084	0.129	-0.035	0.136	0.169	0.131
900462	1.233	0.075	1.106	0.091	0.577	0.073	1.241	0.061
900464	0.217	0.056	0.057	0.067	0.043	0.052	0.239	0.047
900466	0.274	0.102	0.089	0.118	0.097	0.080	0.349	0.079

star	$(B-V)$	$\sigma_{(B-V)}$	$(U-B)$	$\sigma_{(U-B)}$	$(V-R)$	$\sigma_{(V-R)}$	$(V-I)$	$\sigma_{(V-I)}$
900472	0.449	0.157	0.187	0.178	0.192	0.132	0.524	0.135
900473	0.637	0.175	0.178	0.184	0.463	0.152	1.031	0.124
900474	0.402	0.227	0.060	0.233	0.197	0.195	0.518	0.188
900475	0.250	0.054	0.080	0.068	0.062	0.051	0.281	0.045
900476	0.289	0.134	0.159	0.144	0.093	0.154	0.356	0.122
900477	1.155	0.062	0.916	0.081	0.589	0.053	1.253	0.042
900477	1.155	0.062	0.916	0.081	0.589	0.053	1.253	0.042
900480	0.346	0.098	0.171	0.089	0.106	0.095	0.294	0.094
900481	0.427	0.070	0.246	0.100	0.187	0.071	0.505	0.067
900482	0.245	0.052	0.078	0.064	0.061	0.050	0.301	0.045
900485	0.667	0.213	0.303	0.291	0.367	0.172	0.833	0.160
900486	0.312	0.056	0.112	0.067	0.123	0.051	0.393	0.045
900487	0.383	0.141	0.325	0.156	0.128	0.123	0.439	0.127
900488	0.238	0.128	0.095	0.104	-0.036	0.229	0.207	0.112
900490	0.297	0.126	0.347	0.140	0.160	0.132	0.503	0.115
900492	1.156	0.058	0.865	0.076	0.571	0.054	1.216	0.045
900494	0.242	0.054	0.057	0.063	0.056	0.050	0.269	0.045
900498	0.337	0.057	0.236	0.093	0.093	0.054	0.331	0.051
900499	0.154	0.204	0.303	0.275	0.399	0.181	1.176	0.136
900500	1.135	0.063	0.926	0.079	0.598	0.058	1.265	0.050
900502	0.597	0.093	0.149	0.103	0.350	0.089	0.808	0.083
900504	1.178	0.071	1.001	0.101	0.565	0.067	1.234	0.059
900505	0.303	0.065	0.215	0.080	0.062	0.068	0.255	0.067
900506	0.433	0.095	0.287	0.141	0.092	0.098	0.380	0.084
900507	0.256	0.078	0.151	0.089	0.036	0.067	0.264	0.071
900510	0.337	0.067	0.224	0.087	0.102	0.060	0.372	0.061
900512	0.397	0.138	0.261	0.163	0.178	0.129	0.515	0.129
900513	0.411	0.059	0.371	0.067	0.010	0.052	0.383	0.040
900514	1.102	0.065	0.806	0.081	0.573	0.056	1.231	0.047
900516	0.305	0.064	0.080	0.072	0.128	0.060	0.426	0.053
900519	0.467	0.076	0.303	0.135	0.208	0.085	0.532	0.068
900526	0.774	0.073	0.286	0.096	0.525	0.079	1.166	0.061
900529	0.571	0.035	0.450	0.057	0.288	0.040	0.733	0.039
900531	1.181	0.058	0.966	0.079	0.584	0.052	1.245	0.044
900533	0.723	0.127	0.339	0.248	0.377	0.147	0.881	0.122
900535	0.371	0.062	0.235	0.084	0.096	0.060	0.338	0.058
900536	0.637	0.114	0.340	0.257	0.323	0.086	0.774	0.080
900538	0.712	0.122	0.319	0.243	0.396	0.095	0.851	0.095
900539	1.180	0.071	0.898	0.098	0.599	0.059	1.259	0.048
900544	0.616	0.111	0.458	0.248	0.203	0.125	0.605	0.123
900545	0.487	0.107	0.464	0.212	0.173	0.082	0.483	0.108
900546	0.356	0.055	0.121	0.068	0.167	0.055	0.531	0.045
900547	0.381	0.057	0.155	0.074	0.151	0.063	0.467	0.051
900547	0.381	0.057	0.155	0.074	0.151	0.063	0.467	0.051

star	$(B-V)$	$\sigma_{(B-V)}$	$(U-B)$	$\sigma_{(U-B)}$	$(V-R)$	$\sigma_{(V-R)}$	$(V-I)$	$\sigma_{(V-I)}$
900547	0.381	0.057	0.155	0.074	0.151	0.063	0.467	0.051
900548	0.471	0.060	0.298	0.078	0.117	0.067	0.421	0.088
900550	0.364	0.087	0.170	0.089	0.078	0.120	0.380	0.072
900551	0.767	0.248	0.229	0.309	0.353	0.206	0.942	0.170
900552	0.482	0.082	0.404	0.100	0.183	0.084	0.520	0.081
900553	0.612	0.123	0.313	0.230	0.340	0.104	0.789	0.106
900554	0.485	0.219	0.080	0.390	0.364	0.275	1.113	0.194
900555	0.493	0.188	0.317	0.245	0.308	0.192	0.791	0.162
900557	0.598	0.169	0.192	0.390	0.457	0.167	1.088	0.112
900559	0.632	0.253	0.173	0.346	0.441	0.289	1.129	0.205
900560	0.315	0.072	0.181	0.088	0.079	0.060	0.318	0.061
900562	0.581	0.054	0.274	0.069	0.304	0.053	0.725	0.042
900563	0.741	0.140	0.418	0.275	0.430	0.112	0.936	0.112
900564	0.444	0.089	0.194	0.085	0.184	0.098	0.524	0.085
900564	0.444	0.089	0.194	0.085	0.184	0.098	0.524	0.085
900564	0.444	0.089	0.194	0.085	0.184	0.098	0.524	0.085
900565	0.337	0.052	0.158	0.070	0.127	0.049	0.406	0.045
900566	0.265	0.057	0.097	0.074	0.077	0.065	0.308	0.051
900568	0.275	0.058	0.113	0.068	0.073	0.058	0.298	0.054
900569	0.296	0.057	0.131	0.075	0.059	0.055	0.297	0.051
900571	0.328	0.186	-0.093	0.480	0.386	0.218	1.232	0.138
900572	0.328	0.186	-0.093	0.480	0.386	0.218	1.232	0.138
900573	0.761	0.193	0.188	0.252	0.308	0.171	0.794	0.161
900576	0.299	0.052	0.146	0.069	0.074	0.051	0.329	0.045
900578	0.642	0.108	0.358	0.245	0.353	0.100	0.821	0.096
900579	0.431	0.127	0.417	0.234	0.151	0.128	0.444	0.131
900581	0.543	0.122	0.345	0.174	0.211	0.082	0.563	0.085
900584	0.305	0.118	0.240	0.147	0.118	0.123	0.356	0.116
900585	0.404	0.134	0.263	0.162	0.151	0.106	0.493	0.112
900589	0.654	0.146	0.385	0.327	0.368	0.127	0.786	0.130
900590	0.431	0.120	0.286	0.159	0.159	0.136	0.339	0.152
900591	0.314	0.032	0.172	0.052	0.082	0.155	0.390	0.026
900594	0.642	0.299	0.080	0.403	0.425	0.297	1.179	0.213
900596	0.379	0.056	0.227	0.077	0.139	0.059	0.402	0.056
900598	0.348	0.063	0.223	0.082	0.104	0.075	0.350	0.074
900599	1.226	0.062	1.060	0.093	0.607	0.059	1.297	0.049
900600	0.289	0.032	0.168	0.045	0.050	0.025	0.330	0.023
900601	0.277	0.089	0.131	0.095	0.097	0.075	0.305	0.075
900603	0.335	0.052	0.136	0.067	0.132	0.051	0.401	0.045
900604	0.257	0.053	0.110	0.073	0.065	0.055	0.271	0.048
900607	0.338	0.068	0.219	0.087	0.123	0.062	0.355	0.060
900609	0.320	0.142	0.179	0.095	0.028	0.129	0.234	0.128
900610	0.285	0.097	0.235	0.135	0.153	0.096	0.511	0.079
900614	0.281	0.063	0.098	0.081	0.072	0.056	0.289	0.055

star	$(B-V)$	$\sigma_{(B-V)}$	$(U-B)$	$\sigma_{(U-B)}$	$(V-R)$	$\sigma_{(V-R)}$	$(V-I)$	$\sigma_{(V-I)}$
900618	0.470	0.107	0.337	0.108	0.141	0.120	0.462	0.104
900619	0.438	0.080	0.266	0.146	0.168	0.070	0.467	0.073
900622	0.621	0.117	0.380	0.252	0.337	0.124	0.740	0.125
900624	0.228	0.088	0.124	0.082	-0.014	0.076	0.204	0.073
900626	0.619	0.096	0.242	0.184	0.375	0.103	0.861	0.087
900630	0.400	0.091	0.222	0.116	0.166	0.081	0.461	0.075
900631	0.321	0.069	0.148	0.073	0.083	0.103	0.325	0.080
900633	1.263	0.055	1.131	0.075	0.611	0.054	1.308	0.044
900634	0.561	0.088	0.390	0.206	0.292	0.093	0.632	0.089
900636	0.732	0.237	0.224	0.310	0.440	0.224	1.018	0.202
900638	0.313	0.075	0.145	0.085	0.063	0.076	0.294	0.063
900639	0.257	0.048	0.087	0.063	0.094	0.046	0.336	0.039
900641	0.612	0.134	0.415	0.223	0.226	0.090	0.636	0.090
900643	0.455	0.066	0.371	0.061	0.320	0.065	0.815	0.056
900644	0.706	0.214	0.274	0.344	0.299	0.187	0.807	0.171
900645	0.443	0.082	0.368	0.107	0.136	0.078	0.400	0.092
900647	0.351	0.053	0.164	0.068	0.124	0.054	0.398	0.054
900648	0.257	0.055	0.100	0.068	0.069	0.052	0.304	0.047
900649	0.718	0.241	0.204	0.317	0.418	0.181	0.951	0.171
900651	0.416	0.042	0.181	0.058	0.211	0.092	0.515	0.043
900652	0.571	0.157	0.586	0.279	0.195	0.148	0.566	0.125
900653	0.652	0.212	0.289	0.307	0.380	0.191	0.791	0.179
900655	0.318	0.057	0.215	0.079	0.089	0.055	0.331	0.059
900658	0.346	0.050	0.234	0.059	0.118	0.054	0.333	0.044
900663	0.375	0.069	0.246	0.091	0.128	0.065	0.393	0.061
900664	0.242	0.054	0.069	0.067	0.068	0.051	0.273	0.042
900664	0.242	0.054	0.069	0.067	0.068	0.051	0.273	0.042
900665	0.405	0.102	0.504	0.223	0.273	0.088	0.653	0.111
900666	0.384	0.081	0.246	0.095	0.140	0.066	0.447	0.063
900669	0.325	0.069	0.250	0.091	0.064	0.067	0.264	0.068
900674	0.252	0.054	0.091	0.067	0.063	0.051	0.267	0.045
900675	0.532	0.107	0.340	0.133	0.300	0.138	0.692	0.190
900677	0.396	0.245	-0.066	0.457	0.386	0.281	1.170	0.164
900678	0.456	0.061	0.361	0.138	0.193	0.068	0.497	0.060
900679	0.469	0.076	0.365	0.097	0.144	0.080	0.485	0.071
900681	0.513	0.104	0.447	0.177	0.174	0.080	0.511	0.097
900682	0.400	0.069	0.276	0.127	0.146	0.068	0.436	0.059
900683	0.581	0.175	0.196	0.254	0.424	0.198	0.988	0.142
900685	0.692	0.198	0.195	0.243	0.467	0.139	0.923	0.147
900687	0.302	0.057	0.155	0.079	0.099	0.054	0.353	0.048
900688	0.316	0.058	0.156	0.067	0.107	0.058	0.370	0.051
900689	0.547	0.120	0.218	0.190	0.321	0.131	0.782	0.093
900691	0.282	0.064	0.181	0.090	0.049	0.060	0.271	0.050
900695	0.738	0.193	0.248	0.285	0.411	0.130	0.803	0.132

star	$(B-V)$	$\sigma_{(B-V)}$	$(U-B)$	$\sigma_{(U-B)}$	$(V-R)$	$\sigma_{(V-R)}$	$(V-I)$	$\sigma_{(V-I)}$
900696	0.631	0.212	0.238	0.314	0.409	0.209	1.027	0.158
900697	0.692	0.193	0.181	0.243	0.355	0.146	0.838	0.127
900699	0.669	0.090	0.394	0.237	0.211	0.076	0.631	0.092
900702	0.382	0.060	0.268	0.084	0.108	0.067	0.387	0.059
900704	0.468	0.091	0.445	0.192	0.250	0.069	0.596	0.081
900705	0.264	0.056	0.143	0.072	0.070	0.054	0.266	0.053
900705	0.264	0.056	0.143	0.072	0.070	0.054	0.266	0.053
900706	0.533	0.135	0.309	0.201	0.211	0.152	0.574	0.144
900708	0.451	0.091	0.386	0.111	0.177	0.080	0.432	0.076
900711	0.496	0.141	0.198	0.331	0.375	0.138	1.006	0.101
900714	0.681	0.148	0.202	0.263	0.346	0.159	0.782	0.126
900715	0.462	0.102	0.367	0.128	0.166	0.139	0.568	0.110
900716	0.267	0.052	0.138	0.072	0.052	0.051	0.285	0.045
900717	0.597	0.243	0.207	0.304	0.390	0.206	0.926	0.180
900718	0.372	0.214	-0.039	0.507	0.365	0.260	1.112	0.166
900719	0.298	0.050	0.141	0.069	0.080	0.055	0.348	0.044
900721	0.642	0.101	0.367	0.263	0.380	0.092	0.744	0.156
900722	0.341	0.071	0.186	0.087	0.109	0.076	0.327	0.085
900723	0.617	0.150	0.323	0.279	0.311	0.157	0.678	0.154
900724	0.585	0.094	0.488	0.222	0.275	0.082	0.666	0.087
900725	0.437	0.100	0.338	0.103	0.168	0.095	0.464	0.100
900726	0.497	0.244	0.079	0.424	0.366	0.273	1.062	0.197
900728	0.712	0.193	0.282	0.271	0.365	0.191	0.845	0.154
900731	1.098	0.063	0.873	0.093	0.568	0.063	1.206	0.051
900736	0.566	0.054	0.235	0.069	0.324	0.054	0.746	0.041
900738	0.602	0.100	0.411	0.225	0.179	0.114	0.561	0.112
900741	0.401	0.101	0.422	0.118	0.273	0.116	0.711	0.097
900744	0.370	0.072	0.256	0.087	0.137	0.093	0.481	0.060
900746	0.352	0.313	0.321	0.524	0.511	0.225	1.347	0.196
900748	0.742	0.155	0.454	0.270	0.223	0.101	0.710	0.106
900752	0.282	0.054	0.101	0.068	0.104	0.052	0.352	0.042
900753	0.268	0.061	0.126	0.070	0.040	0.062	0.262	0.056
900754	0.543	0.130	0.468	0.243	0.284	0.100	0.668	0.095
900757	0.411	0.115	0.288	0.156	0.183	0.111	0.421	0.102
900758	0.508	0.309	0.055	0.483	0.366	0.342	1.126	0.235
900762	0.251	0.052	0.108	0.071	0.069	0.053	0.285	0.046
900764	0.290	0.062	0.233	0.082	0.074	0.061	0.298	0.061
900766	0.429	0.063	0.323	0.079	0.147	0.062	0.413	0.070
900769	0.602	0.187	0.229	0.239	0.393	0.192	0.946	0.149
900773	0.283	0.250	-0.096	0.536	0.361	0.268	1.222	0.206
900774	0.421	0.085	0.329	0.157	0.140	0.090	0.379	0.090
900776	0.575	0.120	0.433	0.252	0.244	0.095	0.624	0.111
900777	0.622	0.145	0.483	0.220	0.189	0.181	0.622	0.142
900779	0.442	0.112	0.333	0.179	0.135	0.086	0.426	0.073

star	$(B-V)$	$\sigma_{(B-V)}$	$(U-B)$	$\sigma_{(U-B)}$	$(V-R)$	$\sigma_{(V-R)}$	$(V-I)$	$\sigma_{(V-I)}$
900780	0.262	0.061	0.144	0.084	0.038	0.062	0.279	0.059
900781	0.642	0.174	0.201	0.255	0.383	0.171	0.841	0.159
900783	0.613	0.180	0.242	0.275	0.357	0.164	0.818	0.176
900785	0.618	0.140	0.290	0.262	0.353	0.158	0.817	0.130
900787	0.626	0.114	0.528	0.207	0.278	0.117	0.595	0.102
900787	0.626	0.114	0.528	0.207	0.278	0.117	0.595	0.102
900789	0.505	0.122	0.279	0.220	0.186	0.107	0.511	0.109
900791	0.705	0.182	0.018	0.424	0.388	0.192	1.040	0.126
900794	0.666	0.150	0.248	0.280	0.419	0.127	0.978	0.125
900795	0.210	0.053	-0.002	0.064	0.027	0.050	0.238	0.042
900798	0.628	0.140	0.248	0.251	0.295	0.151	0.752	0.135
900801	0.540	0.240	0.140	0.264	0.264	0.202	0.703	0.195
900802	0.256	0.057	0.022	0.070	0.051	0.059	0.295	0.053
900806	0.426	0.095	0.214	0.151	0.080	0.076	0.339	0.089
900807	0.740	0.117	0.292	0.257	0.353	0.108	0.853	0.107
900810	0.482	0.111	0.306	0.129	0.202	0.102	0.493	0.093
900815	0.464	0.069	0.155	0.089	0.181	0.079	0.511	0.062
900817	0.618	0.145	0.310	0.262	0.341	0.142	0.780	0.141
900818	0.784	0.120	0.366	0.270	0.452	0.109	1.007	0.099
900819	0.381	0.090	0.175	0.116	0.109	0.086	0.349	0.069
900822	0.309	0.075	0.193	0.086	0.078	0.061	0.334	0.061
900823	0.595	0.242	0.127	0.320	0.373	0.256	0.974	0.208
900826	0.533	0.099	0.347	0.172	0.208	0.092	0.577	0.093
900828	0.483	0.087	0.297	0.107	0.155	0.082	0.499	0.080
900832	0.466	0.105	0.293	0.160	0.200	0.094	0.488	0.087
900834	1.117	0.062	0.854	0.087	0.558	0.057	1.213	0.045
900835	1.006	0.056	0.632	0.073	0.548	0.050	1.191	0.041
900839	0.275	0.053	0.055	0.069	0.077	0.050	0.340	0.042
900840	0.431	0.071	0.221	0.114	0.125	0.070	0.436	0.072
900842	0.460	0.098	0.254	0.155	0.165	0.082	0.478	0.099
900847	0.270	0.057	0.047	0.067	0.051	0.054	0.286	0.051
900851	0.524	0.093	0.491	0.231	0.217	0.086	0.488	0.097
900858	0.260	0.054	0.093	0.069	0.052	0.051	0.275	0.044
900864	0.604	0.141	0.275	0.289	0.331	0.122	0.762	0.118
900865	0.646	0.150	0.270	0.271	0.352	0.148	0.787	0.149
900867	0.576	0.106	0.279	0.242	0.307	0.105	0.720	0.106
900870	0.404	0.072	0.172	0.087	0.158	0.059	0.438	0.057
900872	0.541	0.173	0.177	0.194	0.354	0.187	0.852	0.168
900874	0.444	0.098	0.289	0.119	0.149	0.083	0.446	0.092
900877	0.732	0.138	0.341	0.264	0.416	0.125	0.887	0.147
900881	0.661	0.093	0.225	0.135	0.262	0.105	0.715	0.068
900882	0.232	0.053	0.050	0.064	0.050	0.049	0.272	0.045
900884	0.678	0.171	0.247	0.276	0.359	0.129	0.717	0.139
900887	0.609	0.142	0.250	0.274	0.328	0.110	0.767	0.101

star	$(B-V)$	$\sigma_{(B-V)}$	$(U-B)$	$\sigma_{(U-B)}$	$(V-R)$	$\sigma_{(V-R)}$	$(V-I)$	$\sigma_{(V-I)}$
900888	0.311	0.074	0.186	0.083	0.099	0.064	0.344	0.058
900889	0.707	0.056	0.305	0.066	0.398	0.052	0.881	0.042
900892	0.215	0.054	0.052	0.070	0.025	0.049	0.230	0.044
900897	0.422	0.137	0.241	0.137	0.127	0.123	0.363	0.165
900898	0.301	0.052	0.109	0.064	0.103	0.050	0.376	0.043
900899	0.263	0.061	0.114	0.070	0.061	0.056	0.280	0.059
900901	0.517	0.250	0.110	0.461	0.408	0.263	1.137	0.181
900906	0.313	0.058	0.129	0.084	0.087	0.055	0.361	0.048
900907	0.175	0.053	-0.005	0.067	0.014	0.048	0.208	0.041
900909	0.686	0.215	0.166	0.266	0.407	0.190	0.910	0.183
900911	0.697	0.322	-0.013	0.393	0.438	0.249	0.965	0.221
900916	0.103	0.255	-0.024	0.438	0.379	0.206	1.254	0.158
900919	0.303	0.051	0.076	0.065	0.110	0.052	0.363	0.045
900921	0.661	0.138	0.221	0.253	0.356	0.104	0.794	0.104
900922	0.305	0.107	0.197	0.100	0.084	0.150	0.385	0.097
900927	0.581	0.185	0.235	0.249	0.429	0.169	0.922	0.166
900929	0.689	0.114	0.246	0.250	0.403	0.102	0.886	0.095
900930	0.382	0.067	0.167	0.093	0.161	0.065	0.417	0.062
900934	0.804	0.087	0.310	0.252	0.248	0.084	0.663	0.088
900935	0.294	0.049	0.121	0.066	0.078	0.050	0.297	0.043
900937	0.330	0.067	0.210	0.086	0.140	0.064	0.388	0.062
900940	0.588	0.106	0.279	0.243	0.319	0.112	0.754	0.104
900942	0.513	0.130	0.394	0.195	0.185	0.097	0.490	0.107
900947	0.282	0.051	0.106	0.068	0.081	0.050	0.323	0.042
900949	0.497	0.164	0.344	0.150	0.247	0.200	0.754	0.130
900951	0.229	0.056	0.089	0.068	0.014	0.059	0.226	0.048
900952	0.317	0.061	0.181	0.082	0.095	0.056	0.336	0.057
900953	0.628	0.117	0.301	0.244	0.366	0.095	0.788	0.111
900958	0.094	0.256	0.072	0.358	0.393	0.184	1.334	0.149
900959	0.625	0.111	0.244	0.241	0.359	0.105	0.824	0.117
900961	0.549	0.080	0.228	0.143	0.258	0.065	0.609	0.056
900962	0.600	0.238	0.284	0.339	0.409	0.223	1.043	0.183
900963	0.291	0.219	-0.065	0.439	0.383	0.279	1.234	0.191
900967	0.749	0.145	0.266	0.251	0.288	0.137	0.721	0.135
900968	0.325	0.069	0.213	0.085	0.062	0.066	0.264	0.066
900970	0.233	0.052	0.057	0.062	0.055	0.052	0.246	0.047
900972	0.653	0.264	0.211	0.475	0.308	0.302	0.881	0.215
900973	0.525	0.218	0.112	0.350	0.429	0.251	1.087	0.191
900974	0.251	0.057	0.117	0.072	0.053	0.058	0.274	0.045
900976	0.718	0.259	0.184	0.403	0.295	0.309	0.816	0.228
900980	0.379	0.207	-0.032	0.465	0.414	0.235	1.217	0.182
900981	0.315	0.052	0.091	0.065	0.112	0.049	0.365	0.044
900983	0.607	0.117	0.319	0.258	0.338	0.121	0.791	0.111
900984	0.348	0.071	0.215	0.079	0.103	0.073	0.341	0.068

star	$(B-V)$	$\sigma_{(B-V)}$	$(U-B)$	$\sigma_{(U-B)}$	$(V-R)$	$\sigma_{(V-R)}$	$(V-I)$	$\sigma_{(V-I)}$
900985	0.334	0.054	0.142	0.072	0.139	0.049	0.433	0.042
900986	0.274	0.055	0.080	0.068	0.089	0.055	0.337	0.045
900987	0.266	0.051	0.141	0.070	0.062	0.057	0.300	0.042
900990	0.309	0.276	-0.043	0.433	0.331	0.321	1.127	0.197
900991	0.309	0.276	-0.043	0.433	0.331	0.321	1.127	0.197
900992	0.692	0.114	0.323	0.219	0.422	0.102	0.931	0.099
900993	0.430	0.085	0.263	0.106	0.152	0.073	0.485	0.072
900994	0.252	0.053	0.100	0.067	0.057	0.049	0.249	0.045
900995	0.531	0.107	0.483	0.237	0.158	0.110	0.561	0.108
900998	0.526	0.168	0.434	0.276	0.177	0.131	0.547	0.136

Table 5.5: Calibrated magnitudes in *UBVRI* filter with errors, parallax and magnitude *G*

star	V	σ_V	B	σ_B	U	σ_U	R	σ_R	I	σ_I	π	G
900193	13.140	0.047	13.482	0.058	13.719	0.083	13.054	0.053	12.798	0.061	0.672	13.049
900195	11.675	0.031	12.704	0.038	13.413	0.063	11.128	0.030	10.509	0.023	0.628	11.388
900202	14.780	0.060	15.340	0.066	15.615	0.214	14.464	0.072	14.100	0.074	0.650	14.409
900212	12.207	0.038	12.434	0.038	12.484	0.058	12.167	0.037	11.972	0.029	0.670	12.175
900214	11.788	0.021	12.006	0.020	12.042	0.033	11.745	0.024	11.568	0.024	0.686	11.780
900220	13.707	0.050	14.143	0.078	14.415	0.125	13.579	0.070	13.270	0.042	0.665	13.588
900222	14.519	0.078	15.032	0.126	15.425	0.199	14.372	0.091	13.969	0.074	0.692	14.290
900230	14.897	0.114	15.477	0.086	15.825	0.262	14.630	0.102	14.189	0.082	0.619	14.648
900233	12.460	0.039	12.717	0.041	12.818	0.057	12.436	0.040	12.199	0.031	0.667	12.430
900234	11.873	0.037	12.137	0.038	12.256	0.050	11.832	0.037	11.610	0.026	0.646	11.863
900241	12.968	0.086	13.292	0.077	13.614	0.133	12.949	0.121	12.678	0.118	0.700	13.136
900242	12.983	0.052	13.253	0.053	13.453	0.066	12.949	0.054	12.716	0.053	0.659	12.948
900244	14.774	0.076	15.355	0.096	15.600	0.195	14.535	0.119	14.144	0.107	0.689	14.473
900247	14.003	0.125	14.564	0.108	14.816	0.138	13.881	0.158	13.412	0.147	0.606	14.542
900247	14.003	0.125	14.564	0.108	14.816	0.138	13.881	0.158	13.412	0.147	0.622	14.516
900251	13.604	0.061	13.988	0.072	14.246	0.138	13.519	0.089	13.277	0.071	0.702	13.489
900252	14.165	0.056	14.664	0.098	14.963	0.112	13.983	0.052	13.658	0.063	0.683	13.972
900253	15.506	0.103	16.142	0.117	16.410	0.228	15.099	0.094	14.710	0.087	0.678	15.112
900257	14.343	0.104	14.806	0.108	15.159	0.200	14.148	0.079	13.841	0.108	0.674	14.109
900258	12.309	0.046	12.773	0.047	13.010	0.067	12.214	0.046	11.852	0.029	0.692	13.260
900258	12.309	0.046	12.773	0.047	13.010	0.067	12.214	0.046	11.852	0.029	0.612	13.046
900259	11.928	0.033	12.108	0.040	12.125	0.051	11.935	0.034	11.783	0.032	0.683	11.929
900263	11.255	0.079	11.501	0.028	11.557	0.040	11.243	0.152	11.038	0.070	0.700	11.384
900265	14.770	0.083	15.429	0.078	15.755	0.256	14.462	0.070	14.090	0.105	0.671	14.574
900269	16.045	0.184	16.389	0.179	16.300	0.397	15.723	0.202	14.932	0.075	0.687	15.467
900270	13.876	0.046	14.400	0.083	14.644	0.120	13.636	0.053	13.326	0.071	0.676	13.876
900271	14.166	0.069	14.635	0.074	14.923	0.124	13.990	0.062	13.680	0.072	0.659	13.991

star	V	σ_V	B	σ_B	U	σ_U	R	σ_R	I	σ_I	π	G
900274	16.393	0.222	16.575	0.188	16.513	0.303	15.993	0.268	15.132	0.099	0.662	15.603
900275	14.885	0.079	15.600	0.128	15.912	0.274	14.495	0.087	14.115	0.134	0.640	14.525
900278	12.962	0.035	13.235	0.038	13.438	0.062	12.938	0.039	12.724	0.046	0.647	12.938
900281	15.897	0.208	16.343	0.153	16.448	0.375	15.503	0.223	14.858	0.076	0.632	15.333
900282	10.779	0.036	11.656	0.039	12.159	0.054	10.303	0.035	9.724	0.017	0.619	12.629
900285	12.215	0.038	12.485	0.039	12.592	0.052	12.135	0.035	11.892	0.026	0.650	12.171
900293	13.360	0.045	13.687	0.054	13.874	0.069	13.295	0.053	13.059	0.043	0.683	13.273
900301	15.646	0.151	16.220	0.125	16.359	0.238	15.261	0.189	14.697	0.052	0.656	15.209
900302	14.826	0.088	15.483	0.098	15.790	0.224	14.541	0.073	14.093	0.059	0.689	14.550
900304	13.482	0.046	13.889	0.062	14.035	0.064	13.336	0.041	13.070	0.046	0.674	13.384
900305	12.334	0.038	12.616	0.039	12.705	0.064	12.260	0.033	12.041	0.029	0.700	12.309
900307	14.312	0.072	14.703	0.101	14.992	0.090	14.246	0.065	13.959	0.071	0.573	14.171
900309	11.260	0.036	12.450	0.045	13.450	0.072	10.689	0.036	10.030	0.021	0.645	10.957
900310	12.122	0.038	12.333	0.038	12.347	0.051	12.076	0.033	11.860	0.028	0.611	12.134
900311	14.155	0.055	14.632	0.060	14.963	0.091	13.939	0.061	13.718	0.060	0.654	14.108
900314	11.825	0.039	12.074	0.040	12.155	0.054	11.791	0.032	11.563	0.029	0.666	11.856
900317	15.656	0.148	16.304	0.129	16.433	0.225	15.319	0.167	14.754	0.070	0.628	15.261
900319	15.430	0.088	16.097	0.131	16.367	0.236	15.019	0.092	14.555	0.096	0.664	15.044
900320	13.806	0.048	14.238	0.077	14.432	0.120	13.646	0.060	13.349	0.050	0.673	13.673
900321	15.634	0.138	16.233	0.139	16.415	0.188	15.248	0.114	14.652	0.070	0.691	15.269
900323	14.056	0.074	14.600	0.091	14.906	0.126	13.789	0.068	13.433	0.054	0.703	13.855
900324	14.148	0.063	14.745	0.098	15.049	0.120	13.894	0.056	13.503	0.061	0.677	13.955
900328	13.548	0.044	13.965	0.061	14.230	0.107	13.428	0.049	13.132	0.034	0.679	13.459
900329	13.075	0.041	13.405	0.045	13.584	0.069	12.963	0.044	12.695	0.050	0.680	12.976
900337	13.058	0.047	13.371	0.058	13.553	0.071	12.998	0.043	12.781	0.039	0.658	13.002
900338	14.613	0.071	15.159	0.071	15.486	0.230	14.340	0.072	13.925	0.071	0.660	14.313
900339	12.954	0.044	13.289	0.053	13.452	0.070	12.852	0.045	12.580	0.049	0.634	12.881
900340	14.715	0.064	15.339	0.084	15.613	0.233	14.437	0.070	13.991	0.065	0.654	14.498

star	V	σ_V	B	σ_B	U	σ_U	R	σ_R	I	σ_I	π	G
900342	15.856	0.167	16.300	0.132	16.377	0.382	15.491	0.194	14.788	0.066	0.640	15.336
900349	13.179	0.039	13.476	0.054	13.681	0.063	13.130	0.043	12.904	0.045	0.677	13.138
900352	14.305	0.052	14.773	0.077	15.314	0.209	14.092	0.048	13.770	0.065	0.652	14.074
900353	14.791	0.082	15.371	0.091	15.714	0.261	14.491	0.087	14.067	0.091	0.647	14.481
900354	12.946	0.056	13.288	0.056	13.518	0.071	12.868	0.050	12.650	0.040	0.660	12.969
900355	15.674	0.141	16.240	0.145	16.346	0.420	15.249	0.167	14.567	0.078	0.623	15.201
900357	13.569	0.067	13.945	0.079	14.120	0.083	13.487	0.087	13.211	0.046	0.697	13.495
900359	12.055	0.038	12.386	0.042	12.506	0.059	11.943	0.035	11.661	0.029	0.669	12.016
900363	11.225	0.036	11.453	0.041	11.504	0.058	11.174	0.035	10.967	0.025	0.678	11.232
900365	12.880	0.080	13.300	0.052	13.600	0.085	12.787	0.085	12.441	0.069	0.659	14.196
900367	12.856	0.044	13.192	0.042	13.359	0.072	12.797	0.047	12.534	0.049	0.684	15.506
900368	14.250	0.078	14.851	0.105	15.321	0.207	14.109	0.091	13.734	0.081	0.703	14.225
900373	11.329	0.043	12.484	0.043	13.424	0.071	10.781	0.040	10.130	0.023	0.659	11.056
900374	15.046	0.109	15.781	0.172	16.012	0.267	14.674	0.127	14.167	0.094	0.669	14.797
900375	13.503	0.046	13.901	0.066	14.090	0.118	13.357	0.066	13.060	0.040	0.649	13.380
900376	13.657	0.046	14.100	0.069	14.345	0.127	13.484	0.063	13.176	0.048	0.659	13.516
900377	11.104	0.039	11.369	0.038	11.448	0.057	11.044	0.041	10.827	0.027	0.645	11.126
900378	13.633	0.043	14.037	0.063	14.337	0.122	13.526	0.058	13.246	0.042	0.691	13.547
900382	13.795	0.052	14.107	0.062	14.287	0.121	13.713	0.046	13.542	0.066	0.703	15.107
900383	12.535	0.037	12.965	0.038	13.146	0.058	12.375	0.043	12.073	0.029	0.675	12.478
900386	14.507	0.077	15.168	0.082	15.469	0.180	14.289	0.117	13.891	0.059	0.699	14.322
900387	15.333	0.150	15.733	0.105	15.898	0.095	15.005	0.127	14.480	0.026	0.631	15.119
900389	12.194	0.037	12.456	0.040	12.565	0.060	12.112	0.036	11.867	0.032	0.691	12.181
900390	13.591	0.059	14.032	0.076	14.303	0.128	13.426	0.067	13.156	0.078	0.681	13.443
900393	11.542	0.042	11.900	0.042	12.040	0.056	11.395	0.038	11.104	0.027	0.683	11.497
900394	14.440	0.104	14.953	0.103	15.312	0.247	14.194	0.114	13.889	0.143	0.654	14.126
900398	14.129	0.061	14.645	0.099	14.966	0.145	13.916	0.064	13.580	0.068	0.651	13.943
900400	13.590	0.046	14.087	0.060	14.378	0.122	13.383	0.063	13.044	0.051	0.673	13.447

star	V	σ_V	B	σ_B	U	σ_U	R	σ_R	I	σ_I	π	G
900401	10.973	0.023	12.221	0.023	13.294	0.039	10.364	0.019	9.683	0.016	0.669	10.643
900403	12.968	0.041	13.303	0.047	13.485	0.070	12.879	0.050	12.611	0.042	0.654	12.882
900404	10.543	0.040	10.738	0.043	10.776	0.063	10.519	0.037	10.327	0.025	0.702	10.594
900406	15.969	0.116	16.422	0.055	16.501	0.231	15.637	0.137	15.056	0.050	0.582	15.577
900408	14.492	0.070	15.273	0.103	15.642	0.247	14.206	0.078	13.704	0.072	0.678	14.251
900410	12.406	0.038	12.729	0.043	12.872	0.062	12.312	0.038	12.058	0.039	0.601	12.366
900414	11.488	0.042	12.690	0.057	13.656	0.099	10.885	0.042	10.206	0.023	0.637	11.146
900416	13.951	0.040	14.522	0.083	14.775	0.160	13.717	0.061	13.402	0.075	0.690	13.842
900417	14.352	0.135	14.967	0.177	15.213	0.218	14.156	0.118	13.795	0.110	0.688	14.074
900418	13.759	0.052	14.201	0.078	14.458	0.126	13.596	0.057	13.347	0.065	0.605	15.826
900421	11.043	0.029	12.213	0.113	13.263	0.197	10.464	0.025	9.799	0.022	0.623	10.736
900422	11.105	0.131	11.418	0.094	11.649	0.065	11.090	0.045	10.848	0.037	0.654	11.202
900423	13.276	0.070	13.683	0.081	13.985	0.158	13.157	0.108	12.832	0.066	0.635	13.119
900425	12.708	0.046	13.017	0.036	13.183	0.056	12.631	0.049	12.369	0.043	0.610	12.715
900426	13.629	0.056	14.095	0.077	14.376	0.132	13.448	0.072	13.153	0.060	0.627	13.485
900430	14.186	0.136	14.722	0.139	15.199	0.239	13.943	0.116	13.577	0.122	0.662	13.861
900431	14.808	0.125	15.465	0.124	15.868	0.250	14.424	0.113	13.933	0.077	0.683	14.445
900432	14.023	0.075	14.474	0.111	14.823	0.093	13.904	0.104	13.552	0.054	0.638	13.858
900435	11.453	0.037	11.715	0.038	11.794	0.057	11.384	0.036	11.145	0.024	0.664	11.450
900436	15.579	0.150	16.269	0.145	16.462	0.181	15.169	0.141	14.642	0.069	0.621	15.178
900438	12.420	0.035	12.680	0.041	12.790	0.056	12.364	0.045	12.126	0.032	0.665	12.386
900440	12.465	0.036	12.797	0.040	12.945	0.060	12.360	0.036	12.084	0.031	0.668	12.438
900441	16.129	0.277	16.483	0.187	16.830	0.284	15.708	0.189	15.019	0.073	0.573	15.555
900446	12.629	0.064	12.808	0.108	12.916	0.083	12.645	0.066	12.436	0.065	0.666	12.628
900447	12.191	0.037	12.529	0.042	12.701	0.055	12.112	0.035	11.862	0.037	0.672	12.805
900447	12.191	0.037	12.529	0.042	12.701	0.055	12.112	0.035	11.862	0.037	0.675	13.041
900451	12.367	0.039	12.613	0.039	12.706	0.056	12.308	0.053	12.081	0.017	0.670	12.342
900453	13.842	0.048	14.293	0.080	14.630	0.138	13.714	0.056	13.406	0.075	0.638	13.711

star	V	σ_V	B	σ_B	U	σ_U	R	σ_R	I	σ_I	π	G
900454	15.291	0.118	15.958	0.155	16.242	0.188	14.856	0.090	14.367	0.087	0.611	14.972
900455	15.410	0.172	16.065	0.215	16.312	0.206	15.001	0.139	14.459	0.066	0.621	15.189
900457	12.044	0.099	12.257	0.059	12.372	0.051	11.939	0.068	11.638	0.030	0.692	11.961
900458	12.718	0.057	13.064	0.134	13.246	0.068	12.556	0.068	12.209	0.049	0.692	13.205
900458	12.718	0.057	13.064	0.134	13.246	0.068	12.556	0.068	12.209	0.049	0.692	11.961
900459	11.315	0.127	11.558	0.112	11.642	0.064	11.350	0.049	11.146	0.033	0.650	11.472
900462	11.062	0.057	12.295	0.049	13.401	0.076	10.485	0.045	9.821	0.022	0.703	10.767
900464	11.404	0.039	11.621	0.040	11.678	0.054	11.361	0.034	11.165	0.026	0.698	11.418
900466	12.503	0.059	12.777	0.083	12.866	0.084	12.406	0.053	12.154	0.051	0.641	12.380
900472	13.523	0.105	13.972	0.116	14.159	0.135	13.331	0.079	12.999	0.084	0.641	13.293
900473	15.852	0.109	16.489	0.137	16.666	0.123	15.389	0.106	14.821	0.058	0.608	15.329
900474	13.611	0.148	14.013	0.172	14.073	0.157	13.414	0.127	13.092	0.116	0.666	13.172
900475	11.767	0.035	12.017	0.041	12.097	0.054	11.705	0.037	11.486	0.028	0.629	11.754
900476	13.429	0.107	13.718	0.081	13.877	0.120	13.335	0.110	13.073	0.059	0.678	13.360
900477	10.934	0.038	12.089	0.050	13.005	0.064	10.345	0.036	9.682	0.019	0.675	10.677
900477	10.934	0.038	12.089	0.050	13.005	0.064	10.345	0.036	9.682	0.019	0.664	13.690
900480	12.862	0.074	13.208	0.063	13.379	0.063	12.756	0.060	12.568	0.057	0.679	13.616
900481	13.066	0.048	13.493	0.051	13.739	0.086	12.879	0.052	12.561	0.047	0.622	13.377
900482	11.554	0.032	11.798	0.041	11.877	0.049	11.493	0.039	11.253	0.032	0.664	11.512
900485	15.320	0.136	15.987	0.164	16.290	0.241	14.953	0.105	14.487	0.085	0.660	14.951
900486	11.697	0.037	12.008	0.043	12.121	0.051	11.574	0.035	11.303	0.026	0.625	11.654
900487	13.854	0.099	14.238	0.101	14.563	0.119	13.726	0.073	13.415	0.080	0.673	13.662
900488	11.890	0.108	12.128	0.070	12.222	0.078	11.926	0.202	11.682	0.030	0.670	12.010
900490	13.871	0.100	14.168	0.076	14.515	0.117	13.711	0.086	13.368	0.057	0.692	13.644
900492	11.467	0.039	12.623	0.043	13.488	0.063	10.896	0.037	10.251	0.022	0.697	11.180
900494	12.028	0.037	12.270	0.040	12.327	0.049	11.973	0.034	11.759	0.027	0.666	12.010
900498	12.918	0.035	13.255	0.045	13.491	0.082	12.825	0.042	12.587	0.037	0.671	12.861
900499	15.746	0.126	15.900	0.160	16.203	0.224	15.347	0.130	14.570	0.051	0.691	15.198

star	V	σ_V	B	σ_B	U	σ_U	R	σ_R	I	σ_I	π	G
900500	11.472	0.043	12.607	0.045	13.533	0.065	10.874	0.038	10.207	0.025	0.672	11.119
900502	14.872	0.061	15.469	0.069	15.618	0.076	14.521	0.064	14.064	0.056	0.643	14.512
900504	11.156	0.053	12.334	0.046	13.335	0.089	10.591	0.041	9.922	0.025	0.687	10.865
900505	13.381	0.047	13.684	0.045	13.899	0.067	13.319	0.049	13.126	0.047	0.625	13.301
900506	13.663	0.073	14.096	0.061	14.383	0.127	13.571	0.065	13.283	0.041	0.678	13.593
900507	12.555	0.046	12.810	0.064	12.961	0.062	12.519	0.048	12.291	0.054	0.676	12.569
900510	12.933	0.042	13.270	0.052	13.493	0.069	12.831	0.043	12.561	0.045	0.627	12.860
900512	13.722	0.101	14.120	0.095	14.381	0.132	13.544	0.080	13.207	0.081	0.695	13.495
900513	13.927	0.036	14.337	0.047	14.708	0.048	13.917	0.038	13.544	0.019	0.666	11.266
900514	11.511	0.043	12.613	0.049	13.419	0.064	10.938	0.036	10.280	0.019	0.666	11.266
900516	12.108	0.044	12.414	0.047	12.494	0.055	11.980	0.042	11.682	0.030	0.675	12.043
900519	13.724	0.048	14.191	0.060	14.494	0.121	13.516	0.070	13.192	0.048	0.611	13.563
900526	15.331	0.055	16.105	0.048	16.391	0.084	14.806	0.057	14.165	0.026	0.567	15.107
900529	14.131	0.029	14.702	0.020	15.152	0.054	13.843	0.028	13.398	0.026	0.665	13.843
900531	11.325	0.038	12.505	0.043	13.472	0.066	10.741	0.036	10.080	0.023	0.701	11.019
900533	15.252	0.070	15.975	0.106	16.314	0.224	14.875	0.130	14.371	0.100	0.638	14.852
900535	13.125	0.037	13.496	0.050	13.731	0.067	13.029	0.047	12.787	0.044	0.664	13.070
900536	14.837	0.058	15.474	0.098	15.813	0.237	14.514	0.064	14.063	0.056	0.687	14.550
900538	14.587	0.066	15.299	0.103	15.618	0.220	14.191	0.067	13.735	0.068	0.577	14.312
900539	11.627	0.042	12.807	0.057	13.705	0.080	11.028	0.042	10.368	0.023	0.658	11.294
900544	14.538	0.082	15.154	0.075	15.611	0.236	14.335	0.095	13.933	0.091	0.674	14.310
900545	14.159	0.065	14.646	0.085	15.110	0.194	13.986	0.051	13.676	0.086	0.642	13.971
900546	11.530	0.038	11.886	0.040	12.006	0.055	11.363	0.039	11.000	0.024	0.639	11.662
900547	10.999	0.039	11.380	0.041	11.534	0.061	10.848	0.050	10.531	0.032	0.646	11.486
900547	10.999	0.039	11.380	0.041	11.534	0.061	10.848	0.050	10.531	0.032	0.674	12.057
900547	10.999	0.039	11.380	0.041	11.534	0.061	10.848	0.050	10.531	0.032	0.595	14.301
900548	13.741	0.048	14.213	0.036	14.510	0.069	13.624	0.047	13.321	0.073	0.676	13.605
900550	10.961	0.059	11.325	0.064	11.494	0.061	10.883	0.105	10.581	0.042	0.684	11.203

star	V	σ_V	B	σ_B	U	σ_U	R	σ_R	I	σ_I	π	G
900551	15.359	0.138	16.127	0.206	16.356	0.231	15.006	0.154	14.417	0.100	0.632	14.945
900552	13.762	0.062	14.244	0.054	14.648	0.084	13.579	0.057	13.242	0.052	0.672	13.669
900553	14.858	0.072	15.470	0.099	15.784	0.208	14.518	0.076	14.070	0.077	0.658	14.547
900554	15.874	0.181	16.359	0.124	16.439	0.370	15.511	0.207	14.761	0.070	0.670	15.349
900555	14.685	0.129	15.178	0.137	15.495	0.203	14.377	0.142	13.894	0.097	0.653	14.252
900557	15.493	0.103	16.091	0.134	16.284	0.366	15.036	0.131	14.405	0.043	0.624	15.089
900559	15.737	0.188	16.370	0.169	16.542	0.302	15.296	0.219	14.608	0.080	0.642	15.180
900560	12.991	0.043	13.306	0.058	13.488	0.067	12.912	0.042	12.673	0.043	0.645	12.927
900562	10.826	0.037	11.407	0.039	11.682	0.057	10.522	0.039	10.101	0.021	0.683	10.750
900563	15.134	0.077	15.874	0.117	16.292	0.249	14.703	0.081	14.197	0.082	0.704	14.752
900564	12.300	0.073	12.743	0.050	12.938	0.068	12.115	0.065	11.775	0.043	0.626	15.768
900564	12.300	0.073	12.743	0.050	12.938	0.068	12.115	0.065	11.775	0.043	0.620	13.782
900564	12.300	0.073	12.743	0.050	12.938	0.068	12.115	0.065	11.775	0.043	0.677	14.592
900565	12.167	0.034	12.504	0.039	12.662	0.058	12.040	0.035	11.761	0.030	0.682	12.111
900566	11.613	0.043	11.878	0.038	11.974	0.063	11.536	0.049	11.305	0.028	0.660	11.637
900568	11.927	0.043	12.202	0.039	12.315	0.055	11.854	0.039	11.629	0.032	0.697	11.919
900569	12.684	0.034	12.980	0.046	13.111	0.059	12.625	0.043	12.388	0.039	0.639	12.653
900571	16.082	0.123	16.410	0.139	16.317	0.460	15.696	0.179	14.851	0.062	0.679	15.518
900572	16.082	0.123	16.410	0.139	16.317	0.460	15.696	0.179	14.851	0.062	0.679	15.518
900573	14.937	0.124	15.698	0.148	15.886	0.204	14.629	0.117	14.143	0.103	0.586	14.519
900576	11.565	0.035	11.864	0.039	12.010	0.057	11.491	0.037	11.236	0.028	0.700	11.551
900578	14.950	0.067	15.592	0.084	15.950	0.230	14.597	0.074	14.129	0.068	0.704	14.635
900579	14.091	0.084	14.522	0.095	14.939	0.214	13.941	0.097	13.647	0.100	0.669	13.830
900581	14.096	0.056	14.639	0.109	14.984	0.136	13.886	0.060	13.534	0.064	0.637	13.967
900584	13.002	0.092	13.307	0.074	13.547	0.126	12.885	0.083	12.647	0.070	0.653	12.840
900585	13.623	0.090	14.027	0.099	14.291	0.128	13.472	0.056	13.130	0.066	0.653	13.452
900589	15.070	0.090	15.724	0.115	16.109	0.306	14.702	0.090	14.284	0.093	0.679	14.712
900590	13.831	0.079	14.262	0.090	14.548	0.132	13.672	0.111	13.492	0.130	0.680	13.642

star	V	σ_V	B	σ_B	U	σ_U	R	σ_R	I	σ_I	π	G
900591	12.930	0.013	13.244	0.029	13.417	0.044	12.848	0.155	12.540	0.023	0.663	12.875
900594	16.015	0.197	16.657	0.226	16.737	0.334	15.590	0.223	14.836	0.081	0.577	15.367
900596	13.209	0.036	13.588	0.043	13.815	0.064	13.070	0.046	12.807	0.043	0.684	13.130
900598	13.246	0.043	13.594	0.046	13.816	0.068	13.142	0.061	12.896	0.059	0.682	13.132
900599	11.219	0.043	12.445	0.044	13.505	0.082	10.611	0.039	9.922	0.022	0.675	10.888
900601	12.840	0.057	13.117	0.068	13.249	0.066	12.743	0.048	12.535	0.048	0.681	12.720
900603	12.200	0.035	12.534	0.039	12.671	0.055	12.068	0.037	11.799	0.028	0.692	12.150
900604	12.314	0.036	12.571	0.039	12.681	0.062	12.249	0.041	12.043	0.032	0.662	12.275
900607	13.032	0.042	13.370	0.053	13.589	0.069	12.910	0.046	12.678	0.043	0.653	12.943
900609	12.046	0.120	12.366	0.075	12.545	0.058	12.017	0.046	11.811	0.045	0.621	12.139
900610	13.130	0.074	13.416	0.063	13.650	0.120	12.977	0.061	12.619	0.026	0.660	13.022
900614	12.564	0.039	12.845	0.050	12.943	0.063	12.492	0.040	12.275	0.039	0.656	12.511
900618	14.048	0.082	14.518	0.069	14.855	0.083	13.908	0.087	13.586	0.064	0.670	13.933
900619	13.664	0.042	14.102	0.068	14.368	0.129	13.496	0.056	13.197	0.059	0.669	13.536
900622	14.868	0.086	15.489	0.080	15.869	0.240	14.531	0.089	14.128	0.090	0.649	14.536
900624	11.703	0.068	11.931	0.055	12.055	0.060	11.717	0.034	11.499	0.027	0.686	11.776
900626	14.691	0.071	15.310	0.064	15.552	0.172	14.316	0.074	13.829	0.049	0.664	14.361
900630	13.242	0.058	13.642	0.070	13.864	0.093	13.076	0.056	12.781	0.047	0.659	13.086
900631	12.500	0.052	12.821	0.045	12.968	0.057	12.417	0.089	12.174	0.060	0.678	14.435
900633	10.905	0.038	12.169	0.040	13.300	0.063	10.294	0.039	9.597	0.023	0.673	10.568
900634	14.542	0.064	15.103	0.060	15.493	0.197	14.250	0.068	13.911	0.062	0.667	14.343
900636	15.701	0.150	16.433	0.184	16.657	0.249	15.261	0.166	14.682	0.136	0.621	15.240
900638	13.189	0.046	13.502	0.060	13.647	0.060	13.126	0.061	12.895	0.044	0.671	13.100
900639	11.614	0.031	11.872	0.037	11.959	0.051	11.520	0.035	11.278	0.024	0.609	11.586
900641	14.542	0.059	15.155	0.120	15.570	0.188	14.316	0.067	13.906	0.068	0.684	14.305
900643	14.474	0.049	14.929	0.043	15.300	0.043	14.154	0.042	13.659	0.026	0.682	14.185
900644	15.214	0.112	15.920	0.182	16.194	0.292	14.915	0.149	14.407	0.129	0.638	14.857
900645	13.878	0.054	14.321	0.062	14.689	0.088	13.742	0.056	13.478	0.075	0.676	13.728

star	V	σ_V	B	σ_B	U	σ_U	R	σ_R	I	σ_I	π	G
900647	12.409	0.038	12.760	0.037	12.924	0.057	12.285	0.038	12.011	0.038	0.676	12.432
900648	11.692	0.037	11.949	0.041	12.049	0.055	11.623	0.037	11.388	0.029	0.641	11.686
900649	15.291	0.125	16.009	0.206	16.213	0.241	14.873	0.131	14.340	0.116	0.618	14.815
900651	13.737	0.028	14.153	0.032	14.334	0.049	13.526	0.088	13.222	0.033	0.663	13.617
900652	14.316	0.097	14.887	0.123	15.473	0.250	14.121	0.112	13.750	0.078	0.634	15.519
900653	15.275	0.136	15.927	0.163	16.216	0.260	14.895	0.135	14.483	0.116	0.652	14.857
900655	12.891	0.036	13.209	0.044	13.424	0.065	12.802	0.041	12.560	0.047	0.683	12.837
900658	13.425	0.037	13.771	0.034	14.005	0.048	13.307	0.040	13.092	0.024	0.700	13.350
900663	13.394	0.042	13.770	0.054	14.016	0.073	13.266	0.050	13.002	0.044	0.687	13.285
900664	11.402	0.036	11.643	0.040	11.712	0.054	11.333	0.037	11.129	0.022	0.645	11.961
900664	11.402	0.036	11.643	0.040	11.712	0.054	11.333	0.037	11.129	0.022	0.704	12.386
900665	14.767	0.060	15.172	0.082	15.676	0.207	14.494	0.065	14.114	0.093	0.703	14.421
900666	13.512	0.043	13.896	0.068	14.143	0.065	13.372	0.050	13.065	0.046	0.629	13.405
900669	13.077	0.045	13.402	0.053	13.652	0.074	13.013	0.050	12.813	0.051	0.641	13.011
900674	11.900	0.037	12.152	0.039	12.243	0.054	11.837	0.036	11.633	0.026	0.661	11.886
900675	13.716	0.084	14.248	0.067	14.588	0.115	13.416	0.109	13.024	0.171	0.690	13.759
900677	16.023	0.144	16.419	0.198	16.352	0.411	15.637	0.241	14.853	0.079	0.701	15.452
900678	13.623	0.042	14.079	0.044	14.440	0.130	13.430	0.054	13.126	0.043	0.702	13.495
900679	13.849	0.050	14.318	0.057	14.683	0.079	13.705	0.062	13.364	0.051	0.668	13.758
900681	14.256	0.059	14.769	0.085	15.216	0.155	14.082	0.053	13.744	0.076	0.659	14.066
900682	13.553	0.038	13.953	0.058	14.229	0.114	13.408	0.057	13.117	0.045	0.636	13.442
900683	15.791	0.132	16.373	0.114	16.568	0.227	15.367	0.148	14.803	0.053	0.668	15.331
900685	15.593	0.119	16.286	0.158	16.480	0.185	15.126	0.073	14.671	0.086	0.695	15.185
900687	12.529	0.035	12.830	0.045	12.986	0.065	12.430	0.041	12.176	0.033	0.672	12.470
900688	11.975	0.042	12.291	0.040	12.447	0.053	11.868	0.040	11.605	0.030	0.668	11.945
900689	14.779	0.081	15.325	0.089	15.543	0.167	14.458	0.103	13.996	0.046	0.678	14.497
900691	12.748	0.039	13.030	0.051	13.211	0.074	12.698	0.046	12.477	0.032	0.658	12.738
900695	15.340	0.090	16.077	0.171	16.326	0.228	14.929	0.094	14.536	0.096	0.627	14.978

star	V	σ_V	B	σ_B	U	σ_U	R	σ_R	I	σ_I	π	G
900696	15.729	0.133	16.359	0.165	16.597	0.267	15.319	0.160	14.702	0.085	0.620	15.227
900697	15.236	0.102	15.929	0.163	16.109	0.179	14.881	0.104	14.398	0.075	0.681	14.892
900699	14.294	0.059	14.962	0.068	15.356	0.228	14.083	0.048	13.663	0.071	0.651	14.182
900702	13.136	0.036	13.519	0.047	13.787	0.070	13.028	0.056	12.749	0.047	0.678	13.142
900704	14.482	0.051	14.950	0.076	15.396	0.177	14.232	0.046	13.886	0.064	0.675	14.233
900705	11.635	0.039	11.899	0.040	12.042	0.059	11.565	0.038	11.369	0.036	0.647	13.586
900705	11.635	0.039	11.899	0.040	12.042	0.059	11.565	0.038	11.369	0.036	0.695	12.713
900706	14.352	0.105	14.885	0.084	15.194	0.183	14.142	0.110	13.778	0.098	0.675	14.093
900708	13.975	0.056	14.426	0.073	14.813	0.084	13.799	0.058	13.543	0.052	0.690	13.818
900711	15.766	0.082	16.262	0.115	16.460	0.311	15.391	0.111	14.760	0.060	0.659	15.326
900714	15.330	0.080	16.011	0.124	16.212	0.231	14.984	0.137	14.547	0.097	0.645	14.975
900715	14.273	0.085	14.734	0.056	15.101	0.116	14.107	0.110	13.705	0.069	0.639	14.096
900716	12.607	0.032	12.874	0.041	13.012	0.060	12.555	0.039	12.321	0.031	0.644	12.584
900717	15.636	0.140	16.233	0.198	16.439	0.230	15.246	0.151	14.709	0.113	0.668	15.134
900718	15.978	0.152	16.350	0.151	16.311	0.484	15.613	0.211	14.866	0.066	0.653	15.399
900719	12.688	0.030	12.987	0.040	13.128	0.056	12.609	0.047	12.340	0.032	0.657	12.642
900721	15.150	0.069	15.793	0.074	16.159	0.253	14.771	0.061	14.406	0.139	0.656	14.871
900722	13.039	0.054	13.380	0.047	13.566	0.073	12.929	0.053	12.712	0.066	0.657	12.936
900723	15.057	0.088	15.675	0.121	15.997	0.252	14.746	0.130	14.380	0.126	0.692	14.650
900724	14.430	0.056	15.015	0.075	15.503	0.209	14.155	0.060	13.765	0.067	0.597	14.189
900725	14.013	0.071	14.450	0.071	14.788	0.075	13.846	0.064	13.549	0.071	0.636	13.834
900726	15.828	0.185	16.325	0.159	16.405	0.393	15.462	0.201	14.767	0.067	0.619	15.354
900728	15.300	0.102	16.012	0.163	16.293	0.216	14.935	0.161	14.455	0.115	0.666	14.959
900731	10.976	0.042	12.074	0.048	12.947	0.080	10.408	0.047	9.771	0.029	0.690	10.777
900736	9.830	0.036	10.396	0.040	10.631	0.056	9.506	0.041	9.084	0.019	0.683	9.727
900738	14.546	0.072	15.149	0.070	15.560	0.213	14.367	0.089	13.986	0.086	0.703	14.357
900741	14.551	0.094	14.952	0.037	15.375	0.112	14.278	0.069	13.840	0.027	0.616	14.246
900744	13.407	0.047	13.777	0.054	14.032	0.069	13.270	0.080	12.926	0.037	0.676	13.359

star	V	σ_V	B	σ_B	U	σ_U	R	σ_R	I	σ_I	π	G
900746	15.192	0.190	15.544	0.249	15.866	0.461	14.681	0.120	13.845	0.049	0.616	14.629
900748	14.625	0.076	15.367	0.135	15.821	0.234	14.402	0.067	13.914	0.074	0.692	14.468
900752	11.539	0.036	11.821	0.040	11.922	0.055	11.435	0.037	11.187	0.022	0.629	11.521
900753	12.700	0.045	12.968	0.041	13.094	0.057	12.660	0.042	12.438	0.034	0.679	12.686
900754	14.663	0.063	15.206	0.114	15.675	0.215	14.379	0.078	13.995	0.072	0.650	14.324
900757	13.873	0.079	14.285	0.083	14.573	0.132	13.690	0.078	13.452	0.063	0.643	13.695
900758	15.823	0.221	16.331	0.216	16.386	0.432	15.457	0.262	14.697	0.082	0.677	15.191
900762	12.059	0.035	12.310	0.039	12.418	0.059	11.990	0.039	11.774	0.030	0.686	12.028
900764	13.115	0.039	13.405	0.048	13.638	0.067	13.041	0.047	12.817	0.048	0.643	13.043
900766	13.054	0.039	13.483	0.050	13.806	0.061	12.907	0.048	12.641	0.058	0.653	13.401
900769	15.499	0.127	16.101	0.137	16.329	0.196	15.106	0.144	14.553	0.078	0.686	15.044
900773	16.184	0.195	16.466	0.157	16.370	0.512	15.823	0.184	14.962	0.065	0.667	15.490
900774	13.800	0.049	14.221	0.069	14.550	0.141	13.660	0.076	13.421	0.076	0.666	13.657
900776	14.581	0.068	15.156	0.098	15.589	0.232	14.337	0.066	13.957	0.087	0.655	14.323
900777	14.494	0.098	15.116	0.107	15.599	0.192	14.304	0.152	13.872	0.103	0.626	14.356
900779	13.774	0.055	14.216	0.097	14.549	0.151	13.639	0.066	13.347	0.048	0.654	13.643
900780	12.715	0.039	12.978	0.047	13.122	0.069	12.677	0.049	12.437	0.044	0.680	12.667
900781	15.449	0.126	16.091	0.121	16.292	0.224	15.066	0.116	14.608	0.097	0.641	15.049
900783	15.304	0.117	15.918	0.137	16.160	0.238	14.947	0.114	14.486	0.131	0.567	14.852
900785	15.189	0.098	15.806	0.100	16.097	0.242	14.836	0.124	14.371	0.085	0.656	14.786
900787	14.559	0.061	15.184	0.096	15.712	0.183	14.281	0.099	13.964	0.081	0.670	14.512
900787	14.559	0.061	15.184	0.096	15.712	0.183	14.281	0.099	13.964	0.081	0.677	15.754
900789	14.286	0.076	14.790	0.096	15.069	0.198	14.100	0.075	13.775	0.079	0.664	14.073
900791	15.472	0.102	16.178	0.150	16.196	0.396	15.085	0.163	14.432	0.074	0.698	14.998
900794	15.445	0.092	16.111	0.119	16.360	0.253	15.026	0.087	14.467	0.084	0.585	14.947
900795	11.595	0.036	11.805	0.039	11.803	0.051	11.569	0.035	11.358	0.022	0.697	11.593
900798	14.492	0.094	15.120	0.104	15.368	0.229	14.198	0.118	13.740	0.097	0.665	14.120
900801	14.713	0.150	15.253	0.187	15.393	0.186	14.449	0.135	14.010	0.125	0.645	14.134

star	V	σ_V	B	σ_B	U	σ_U	R	σ_R	I	σ_I	π	G
900802	12.134	0.037	12.390	0.043	12.413	0.056	12.083	0.046	11.839	0.038	0.658	12.069
900806	13.721	0.049	14.146	0.081	14.361	0.127	13.640	0.057	13.382	0.074	0.670	13.582
900807	14.788	0.077	15.528	0.088	15.820	0.241	14.435	0.076	13.935	0.074	0.682	14.436
900810	14.039	0.072	14.520	0.084	14.826	0.098	13.836	0.071	13.546	0.058	0.626	13.849
900815	13.438	0.045	13.902	0.053	14.057	0.071	13.257	0.065	12.927	0.043	0.640	13.304
900817	15.039	0.096	15.657	0.109	15.967	0.238	14.698	0.105	14.259	0.103	0.631	14.676
900818	15.066	0.072	15.849	0.096	16.215	0.253	14.613	0.083	14.058	0.069	0.696	14.662
900819	13.539	0.051	13.920	0.073	14.095	0.090	13.430	0.069	13.190	0.045	0.674	13.392
900822	13.223	0.045	13.532	0.060	13.725	0.061	13.145	0.042	12.889	0.041	0.696	13.154
900823	15.647	0.172	16.242	0.170	16.368	0.271	15.274	0.189	14.672	0.117	0.684	15.101
900826	14.303	0.059	14.836	0.079	15.183	0.153	14.095	0.070	13.725	0.072	0.661	14.100
900828	13.873	0.050	14.356	0.071	14.653	0.080	13.718	0.065	13.375	0.062	0.663	13.729
900832	14.101	0.064	14.567	0.083	14.860	0.137	13.901	0.070	13.613	0.059	0.649	13.912
900834	11.539	0.040	12.656	0.047	13.510	0.073	10.981	0.040	10.326	0.020	0.668	11.248
900835	11.305	0.037	12.311	0.042	12.943	0.059	10.757	0.033	10.113	0.018	0.699	11.171
900839	11.358	0.037	11.633	0.038	11.688	0.058	11.281	0.034	11.017	0.021	0.669	11.342
900840	13.414	0.046	13.845	0.054	14.066	0.101	13.290	0.053	12.979	0.055	0.689	13.342
900842	13.752	0.059	14.212	0.078	14.466	0.134	13.588	0.057	13.275	0.080	0.674	13.579
900847	11.879	0.040	12.149	0.041	12.197	0.054	11.828	0.036	11.593	0.032	0.679	15.312
900851	14.274	0.059	14.798	0.072	15.289	0.219	14.057	0.062	13.786	0.077	0.684	14.141
900858	12.490	0.034	12.750	0.042	12.843	0.055	12.439	0.039	12.216	0.028	0.703	12.469
900864	14.983	0.088	15.587	0.110	15.862	0.268	14.652	0.085	14.221	0.078	0.669	14.681
900865	15.315	0.098	15.961	0.114	16.231	0.245	14.962	0.111	14.528	0.112	0.598	14.966
900867	14.790	0.064	15.366	0.084	15.645	0.226	14.482	0.083	14.070	0.084	0.647	14.490
900870	13.047	0.042	13.451	0.059	13.623	0.065	12.889	0.041	12.609	0.038	0.673	12.958
900872	15.047	0.139	15.588	0.103	15.765	0.165	14.693	0.125	14.195	0.094	0.659	14.678
900874	14.003	0.058	14.447	0.079	14.736	0.088	13.854	0.060	13.557	0.071	0.675	13.851
900877	15.133	0.084	15.865	0.109	16.206	0.241	14.717	0.093	14.246	0.120	0.657	14.758

star	V	σ_V	B	σ_B	U	σ_U	R	σ_R	I	σ_I	π	G
900881	14.195	0.058	14.856	0.072	15.082	0.114	13.933	0.087	13.481	0.035	0.647	14.424
900882	11.497	0.035	11.728	0.040	11.778	0.051	11.447	0.034	11.225	0.028	0.672	11.484
900884	14.975	0.093	15.653	0.143	15.899	0.236	14.617	0.090	14.258	0.103	0.613	14.628
900887	14.867	0.074	15.476	0.121	15.726	0.245	14.539	0.081	14.100	0.069	0.686	14.557
900888	13.309	0.043	13.621	0.060	13.806	0.057	13.210	0.048	12.965	0.040	0.661	13.221
900889	10.922	0.038	11.630	0.041	11.935	0.051	10.525	0.035	10.042	0.018	0.576	10.768
900892	12.339	0.034	12.553	0.041	12.605	0.056	12.314	0.035	12.109	0.028	0.654	12.319
900897	14.119	0.092	14.541	0.101	14.782	0.093	13.992	0.082	13.756	0.137	0.673	13.911
900898	11.872	0.034	12.173	0.040	12.282	0.051	11.769	0.037	11.497	0.027	0.662	11.891
900899	12.675	0.040	12.938	0.046	13.052	0.052	12.614	0.039	12.395	0.043	0.660	12.631
900901	15.726	0.171	16.243	0.183	16.354	0.424	15.319	0.200	14.589	0.060	0.660	15.247
900906	12.675	0.038	12.988	0.043	13.117	0.072	12.587	0.040	12.314	0.028	0.703	12.618
900907	11.322	0.036	11.497	0.039	11.492	0.055	11.308	0.033	11.114	0.021	0.606	11.327
900909	15.588	0.132	16.274	0.170	16.440	0.205	15.181	0.136	14.678	0.128	0.677	15.211
900911	15.394	0.175	16.091	0.271	16.078	0.285	14.956	0.177	14.430	0.135	0.682	14.699
900916	16.312	0.145	16.415	0.210	16.391	0.384	15.933	0.147	15.058	0.063	0.610	15.788
900919	11.842	0.035	12.146	0.038	12.221	0.053	11.732	0.038	11.479	0.028	0.692	11.840
900921	15.084	0.074	15.745	0.117	15.966	0.224	14.728	0.073	14.290	0.073	0.674	14.764
900922	13.669	0.079	13.974	0.071	14.170	0.070	13.585	0.127	13.284	0.056	0.679	13.553
900927	15.523	0.139	16.104	0.122	16.339	0.217	15.093	0.097	14.601	0.092	0.653	15.126
900929	14.995	0.070	15.683	0.091	15.929	0.232	14.591	0.074	14.109	0.064	0.591	14.631
900930	13.509	0.042	13.891	0.053	14.058	0.077	13.348	0.050	13.092	0.046	0.650	13.400
900934	14.578	0.058	15.382	0.065	15.692	0.244	14.330	0.061	13.915	0.066	0.641	14.496
900935	12.188	0.034	12.482	0.036	12.602	0.056	12.110	0.037	11.890	0.027	0.682	12.179
900937	13.123	0.042	13.453	0.052	13.663	0.068	12.983	0.049	12.735	0.045	0.677	13.049
900940	14.869	0.071	15.457	0.078	15.735	0.230	14.550	0.086	14.115	0.076	0.632	14.534
900942	14.215	0.073	14.729	0.108	15.123	0.163	14.030	0.064	13.725	0.078	0.668	14.020
900947	11.601	0.035	11.882	0.038	11.988	0.056	11.520	0.036	11.278	0.023	0.692	11.597

star	V	σ_V	B	σ_B	U	σ_U	R	σ_R	I	σ_I	π	G
900949	14.070	0.119	14.566	0.112	14.910	0.100	13.823	0.160	13.316	0.052	0.636	13.853
900951	12.567	0.038	12.797	0.041	12.886	0.055	12.554	0.045	12.341	0.029	0.704	12.559
900952	12.880	0.036	13.197	0.049	13.378	0.065	12.786	0.043	12.545	0.044	0.660	12.811
900953	15.072	0.064	15.700	0.098	16.000	0.224	14.706	0.070	14.284	0.091	0.626	14.723
900958	16.284	0.122	16.378	0.225	16.450	0.279	15.891	0.138	14.950	0.087	0.633	15.554
900959	15.231	0.077	15.856	0.080	16.100	0.228	14.872	0.072	14.407	0.088	0.662	14.857
900961	13.719	0.043	14.268	0.068	14.495	0.126	13.461	0.049	13.109	0.035	0.658	13.543
900962	15.800	0.154	16.401	0.182	16.685	0.286	15.391	0.161	14.757	0.099	0.647	15.275
900963	16.153	0.179	16.444	0.127	16.379	0.420	15.771	0.214	14.919	0.068	0.675	15.522
900967	14.800	0.105	15.549	0.099	15.815	0.230	14.512	0.088	14.079	0.084	0.620	14.608
900968	13.363	0.045	13.688	0.052	13.901	0.067	13.301	0.047	13.099	0.048	0.681	13.284
900970	11.390	0.038	11.623	0.035	11.680	0.051	11.335	0.035	11.144	0.026	0.668	11.438
900972	15.936	0.187	16.589	0.187	16.800	0.436	15.628	0.237	15.055	0.106	0.635	15.205
900973	15.958	0.172	16.483	0.133	16.595	0.324	15.529	0.182	14.871	0.082	0.689	15.412
900974	12.452	0.036	12.704	0.044	12.820	0.056	12.400	0.046	12.178	0.028	0.695	12.414
900976	15.959	0.194	16.677	0.172	16.862	0.365	15.664	0.241	15.143	0.121	0.687	15.244
900980	16.005	0.146	16.384	0.147	16.352	0.441	15.591	0.185	14.788	0.109	0.683	15.376
900981	11.899	0.034	12.214	0.039	12.304	0.052	11.787	0.035	11.534	0.028	0.646	11.862
900983	14.923	0.078	15.530	0.087	15.849	0.242	14.585	0.092	14.133	0.078	0.689	14.557
900984	13.302	0.051	13.651	0.049	13.866	0.063	13.199	0.052	12.961	0.044	0.650	13.213
900985	11.762	0.035	12.095	0.041	12.237	0.059	11.623	0.035	11.329	0.023	0.629	11.713
900986	11.476	0.038	11.750	0.039	11.829	0.056	11.386	0.039	11.139	0.025	0.696	11.456
900987	12.588	0.031	12.854	0.040	12.995	0.057	12.525	0.048	12.288	0.028	0.678	12.536
900990	15.978	0.188	16.287	0.202	16.243	0.383	15.647	0.260	14.851	0.061	0.668	15.354
900991	15.978	0.188	16.287	0.202	16.244	0.383	15.647	0.260	14.851	0.061	0.668	15.354
900992	15.170	0.075	15.863	0.086	16.186	0.201	14.748	0.069	14.239	0.065	0.663	14.941
900993	13.402	0.053	13.832	0.067	14.095	0.082	13.250	0.050	12.917	0.049	0.632	13.318
900994	11.825	0.034	12.077	0.040	12.177	0.053	11.768	0.035	11.575	0.030	0.642	11.815

star	V	σ_V	B	σ_B	U	σ_U	R	σ_R	I	σ_I	π	G
900995	14.525	0.075	15.056	0.076	15.539	0.224	14.367	0.080	13.964	0.078	0.683	14.269
900998	14.449	0.096	14.976	0.137	15.410	0.239	14.272	0.089	13.902	0.097	0.695	14.169

Bibliography

Bennett, J. O., Donahue, M., Schneider, N., & Voit, M. 2019, *The Cosmic Perspective* (9th ed.). Boston: Pearson.

Bertelli, G., Fagotto, F., Bressan, A., Chiosi C. 1994, *Evolutionary sequences of stellar models with new radiative opacities*, Astronomy & Astrophysics, v. 105, p. 29.

Cagaš P. 2025, *SIPS – Software for Image Processing and Simulation*, verze 4.2.3, 2025. access: https://www.gxccd.com/cat?id=146&lang=405

Casamiquela, L.; Blanco-Cuaresma, S.; Carrera, R.; Balaguer-Núñez, L.; Jordi, C.; Anders, F.; Chiappini, C.; Carbajo-Hijarrubia, J.; Aguado, D. S.; del Pino, A.; Díaz-Pérez, L.; Gallart, C.; Pancino, E. 2019, *OCCASO – III. Iron peak and α elements of 18 open clusters. Comparison with chemical evolution models and field stars*, Monthly Notices of the Royal Astronomical Society, v. 490, p. 1821–1842.

Ferreira, F. A.; Santos, J. F. C.; Corradi, W. J. B.; Angelo, M. S.; Maia, F. F. S. 2025, *Open cluster age calibration from colour–magnitude morphological indices using Gaia DR3 data*, Monthly Notices of the Royal Astronomical Society, v. 539, p. 265–281.

Roger Freedman, Robert Geller, William J. Kaufmann. 2019, *Universe* (11th ed.).

Harmanec, P. & Horn, J. 1998, Journal of Astronomical Data, 4, CD-ROM file 5

Kalirai, J. S., Richer, H. B., Reitzel, D., Hansen, B. M. S., Rich, M., Fahlman, G. G., Gibson, B. K., & Ted von Hippel. 2004, *The initial-final mass relationship: spectroscopy of white dwarfs in NGC 2099 (M37)*, Astrophys.J. 618, L123-L128.

Kang, Y. B.; Kim, S.-L.; Rey, S.-C.; Lee, C.-U.; Kim, Y. H.; Koo, J.-R.; Jeon, Y.-B. 2007, *Variable Stars in the Open Cluster NGC 2099 (M37)*, The Astronomical Society of the Pacific, v. 119, n. 853.

Kiss, L. L.; Szabó, Gy. M.; Sziládi, K.; Furész, G.; Sárneczky, K.; Csák, B. 2001, *A variable star survey of the open cluster M 37*, Astronomical Journal, v. 376, p. 561-567.

Landolt, A. U. 2013, *UBVRI photometric standard stars around the sky at +50 deg declination*, Astronomical Journal, v. 104, p. 340-371.

Mermilliod, J.-C., Huestamendia, G., del Rio, G., & Mayor, M. 1995, *Red giants in open clusters. V. NGC 2099*, Astronomy and Astrophysics, v. 307, p. 80.

Nilakshi and R. Sagar. 2002, *A comprehensive study of the rich open star cluster NGC 2099 based on deep BVI CCD observations*, Astronomy and Astrophysics, v. 381, p. 65-76.

Sarajedini, A., Brandt, K., Grocholski, A. J., Tiede, G. P. 2004, *WIYN open cluster study. XIX. Main-sequence-fitting distances to open clusters using V-K color-magnitude diagrams*, Astronomical Journal, v. 127, p. 991-999.

Savage, B. D., Mathis, J. S. 1979, *Observed properties of interstellar dust*, Annual review of astronomy and astrophysics, v. 17, p. 73-111.

Velčovský Jaroslav 2016, *Complex study of the open cluster NGC 2281*, Diploma Thesis, Masaryk University, Brno

West, Frederick R. 1967, *Photographic Photometry of the Galactic Cluster M37*, Astrophysical Journal Supplement, v. 14, p.359.

Online sources

[e1] : http://pleiadi.pd.astro.it

[e2] : https://www.flickr.com/photos/144614754@N02/28147563947/

[e3] : https://www.space.com/pleiades.html

[e4] : http://www.astrophoton.com/trumpler_class.htm

[e5] : https://www.cosmos.esa.int

[e6] : https://ru.wikipedia.org/wiki/à_ľ__ľť

[e7] : https://www.researchgate.net

[e8] : https://www.skyledge.net/Messier36-hop.htm

[e9] : https://www.go-astronomy.com/messier.php?Messier=M37

[e10] : https://www.messier-objects.com/messier-36-pinwheel-cluster/

[e11] : https://www.messier-objects.com/messier-38-starfish-cluster/